Ru-based catalysts for proton exchange membrane water electrolysers: The need to look beyond *just another catalyst*

Shailendra K. Sharma [a], Chang Wu [a], Niall Malone [b], Laura J. Titheridge [a], Chuan Zhao [c], Prasanth Gupta [b,d], Hicham Idriss [e], John V. Kennedy [b,d], Vedran Jovic [b,d,f,*], Aaron T. Marshall [a,d]

[a] *Department of Chemical and Process Engineering, University of Canterbury, Christchurch, 8041, New Zealand*
[b] *Earth Resources and Materials, Institute of Geological and Nuclear Science, Lower Hutt, 5010, New Zealand*
[c] *School of Chemistry, The University of New South Wales, Sydney, New South Wales, 2052, Australia*
[d] *The MacDiarmid Institute for Advanced Materials and Nanotechnology, Wellington, 6012, New Zealand*
[e] *Karlsruhe Institute of Technology (KIT), 76344, Eggenstein-Leopoldshafen, Germany*
[f] *Department of Physics, Boston University, 590 Commonwealth Avenue, Boston, MA, 02215, USA*

A B S T R A C T

Ruthenium (Ru-) based electrocatalysts have historically shown the highest activity for the oxygen evolution reaction in green H_2 production by PEM-based water electrolysis. However, their instability under industrially relevant operating conditions makes the considerably more expensive and scarcer Ir/IrO_2-based electrocatalysts the materials of choice for industrial use – an important technical bottleneck that contributes to the high levelized-cost of green H_2. Despite decades of research, meeting the 'Key Performance Indicators' of industrial systems with Ru/RuO_2-based electrocatalysts is not yet possible, with an in-depth understanding of the engineering strategies and their induced effects still at an early stage. Framing our review from the perspective of a PEM water electrolyser, and the demands that the operating environment puts on the core components, we focus on the state-of-the-art Ru-based electrocatalysts and the physicochemical properties that were used to optimise performance (decrease overpotential and prolong stability). Further, we highlight that due to the intrinsic heterogeneity of the electrocatalysts, an improvement to a certain figure of merit, e.g., stability or activity, is a complex combination of various interlinked factors. We find that most research efforts focus on electrocatalyst preparation via trial-and-error methods and evaluation at low currents densities in short durations. We discuss the obstacles such an approach presents on standardization of results in individual studies, across the community and on the extraction of industrially relevant information. Also, our discussion highlights potential failure mechanisms and development strategies that may maximise the likelihood of success in an applied scenario. Our review underscores the urgent need for electrocatalyst synthesis and testing under more standardized (and closer to applied) conditions if the goal is to develop an industrially relevant material.

1. Introduction

1.1. The oxygen evolution reaction challenge, Ir- and Ru-based electrocatalysts

In hydrogen (H_2) production through a proton exchange membrane water electrolyser (PEM-WE, described extensively within prominent reports) [1–4], the oxygen evolution reaction (OER) at the anode is complemented by the hydrogen evolution reaction (HER) at the cathode. The OER is a kinetically sluggish process compared to the HER and requires a higher overpotential (η), as discussed in many reports [2,5]. To maintain stability under the operating conditions of a PEM-WE, noble metal-based electrocatalysts (with simultaneously excellent intrinsic activity towards the OER) are required.

Iridium and iridium dioxide (Ir-/IrO_2)-based materials exhibit near-optimal activity for the OER and are the only stable electrocatalysts available for commercial-scale PEM electrolysers [1,6,7]. However, their scarcity presents a true bottleneck in scaling up H_2 production to terawatt-level capacity [8–10]. Ru-based catalysts, and in particular RuO_2, are a significantly cheaper (ca. 10 × lower in price) and more abundant alternative to IrO_2 [11]. According to the theoretical 'volcano' plot reported by Nørskov et al. [12], RuO_2 is the most active pure metal oxide electrocatalyst for the OER due to its optimal binding energy with the reaction intermediates [13–15]. However, its dissolution rates are more than an order of magnitude higher than IrO_2 under acidic conditions [16,17], and are reported to vary greatly depending on the composition of the material, the pre-/post-treatment conditions and the operating conditions [17,18]. The low stability of the material remains the main hurdle limiting its implementation in a PEM-WE [11,19].

* Corresponding author. Earth Resources and Materials, Institute of Geological and Nuclear Science, Lower Hutt, 5010, New Zealand.
E-mail address: v.jovic@gns.cri.nz (V. Jovic).

1.2. Attempts, and rational approaches, to improve Ru-based electrocatalysts

Attempts have been made to improve the activity and stability of RuO_2 (rutile structure) and other Ru-based structures, e.g., ruthenate, perovskite, pyrochlore, and Ru-single atom systems [20–22], through alloying, sometimes without considering the immiscibility gap between the elements [14,23,24,24–47]. Given the 84 stable elements in the periodic table that can be used for alloying, a large number of studies are conducted [48–54]. Many of them evaluate the developed poly(nano/-micro-)crystalline electrocatalyst in an aqueous 3-electrode (half) cell, reporting overpotentials at 10 mA cm ^{2} over short time periods without the use of a reliable baseline for comparison amongst the community [55]. Efforts to study these 'applied' electrocatalysts are usually justified by a need to improve performance (activity and stability), and to understand underpinning reason for an enhancement(s) – all in pursuit of developing more affordable anodes for PEM electrolysers.

However, the "So What?" factor [56] is often missing in the quest for a new electrocatalyst; Approaches to synthesise an applied material are dominated by trial-and-error attempts [49–54]. These synthesis methods do not always enable precise control of atom-specific active sites, rather producing poly(nano/micro-)crystalline materials with differing structural, compositional and electronic properties, that are further modified under experimental conditions [57–60]. Other aspects (e.g., the electrode preparation method, its physical properties along the testing protocol) also contribute to the electrochemical response. If the material is unstable in an aqueous half-cell over short time periods and at low current densities, then one may wonder whether adding another electrocatalyst based on a permutation and/or combination of elements contributes meaningly to PEM-WE development.

If the goal is to 'understand underpinning reasons for enhancement', as stated above, a more rational approach is to study the catalyst's functional properties at a level where heterogeneity is minimised and to use this data to fine-tune its performance. Single crystals or epitaxial films enable optimisation at such a level via a bottom-up approach combining theoretical and empirical studies. If, however, the goal, is to develop an industrially relevant catalyst (where understanding fundamental insights is not vital), then screening of the poly(nano/micro-) crystalline electrocatalyst should be rigorous compared to the currently used approaches to report activity and stability. Specifically, to stand out more than just another electrocatalyst, the new electrocatalyst should compete with state-of-the-art Ir-based materials in a half cell and in a PEM cell that emulates industrial operating conditions (expanded on below and in Section 2.1). In the latter case, the electrode architecture, operating conditions, and hydrodynamics are different compared to that in a half cell. Thus, the ability to translate or scale the material between the two testing environments should be verified – a key step in which complexity is underestimated [61–68]. Rotating disk electrode testing for example can overestimate the activity, and underestimate the stability, and differences between Ir and IrO_2 catalysts compared to when they are tested within an electrolyser [69]. The number of studies evaluating electrocatalysts under conditions simulating those in present day or future PEM-WE systems – i.e. in MEAs that are integrated in a cell (e.g. ≥25 cm^2) or stack, at current densities (>1 A cm ^{2}), temperatures (60–80 °C), ambient or partially elevated pressures, and durations (2000–8000 h) tending toward those described in Section 2.1 – coincidently, also remains low. This is all expanded on in later sections.

1.3. Are electrocatalysts for the OER getting better?

We will note briefly here that the number of scientific articles relating to Ir- and Ru-based OER electrocatalysts is increasing rapidly, as shown in Fig. 1 (adapted from the work of Alia [70]). The figure also compares cell voltages of PEM systems operated at 1 A cm ^{2} from randomly selected studies published since the 1970s (the data is summarised in **Appendix 1**) against commercial PEM-WE cell voltage ranges [71,72]. Most of the anode catalysts that are tested in PEM cells for 'long' periods are based on Ir- and Ru-oxides. After an initial improvement in the overall cell voltage, the value at 1 A cm ^{2} has not improved significantly despite the surge in OER electrocatalysts being reported. It should be noted that these studies do not all use cathodes, membranes, porous transport layers (PTLs) or experimental conditions (e.g., temperature, pressure, electrode area, compression, etc.) that are consistent with industrial settings. Due to these caveats, the search for newer anode materials is not being translated into better PEM-WE systems.

2. Requirements for OER electrocatalysts in PEM water electrolysers

2.1. Industrial targets for PEM-WE OER electrocatalysts

Three critical merits of an electrocatalyst are activity, durability, and (low) cost. For currently installed systems, the capital expenditure

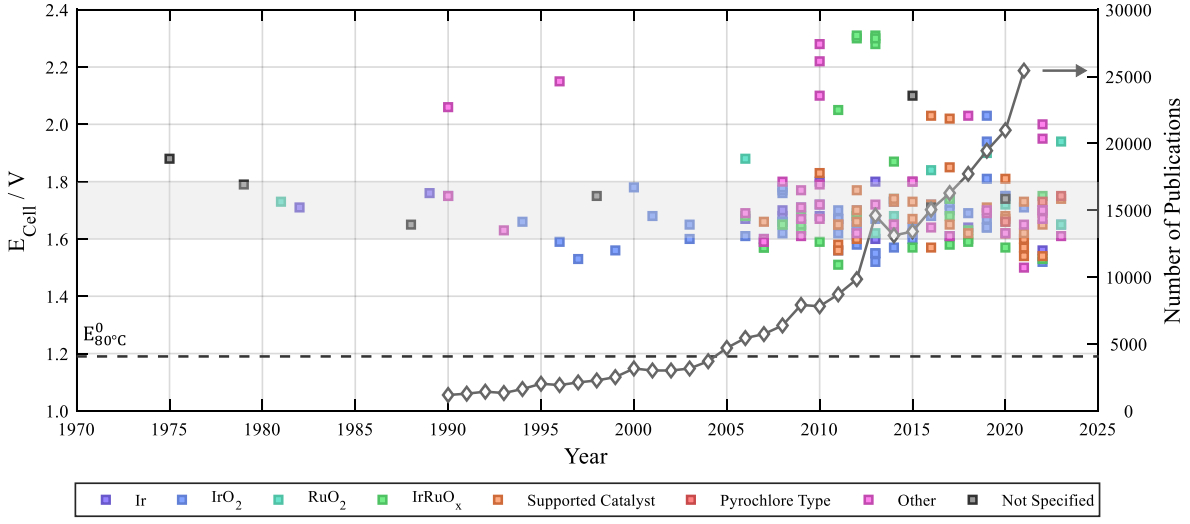

Fig. 1. Cell voltages at 1 A cm^{-2} reported from PEM-WE in literature (summarised in Appendix 1) and the number of papers reporting electrocatalysts for the OER is from the work of Alia [70]. In the plot, 'Other' is also an Ir-based catalyst (see Appendix 1). The grey shaded region represents proposed target voltages at up to 3 A cm^{-2}.

(CAPEX) contribution of the anodic electrocatalyst to the stack is 10–15 % (with electrocatalyst loadings of ~2–5 mg cm ^{2}) [71]. More importantly, noble metal supply (particularly Ir) cannot keep up with increasing electrolyser size capacities [1,70,73]. Thus, projected mass loadings of <0.5 mg cm ^{2} (by 2030) and ~0.1 mg cm ^{2} or below (by 2050) have been suggested to meet future H_2 production demands by improvements of the membrane electrode assembly (MEA), catalyst layer and catalyst itself, the latter by independent development in half cells [10,71,74–76]. The activity and stability targets for PEM-WE systems are also challenging; A cell voltage of 1.6–1.8 V at 3 A cm ^{2} (Fig. 1) with a degradation rate of 2–2.3 mV kh ^{1} and a total lifetime of 80 khr by 2030 have been proposed [25,71,72,77–81].

The electrocatalyst stability particularly must not be an issue, as we will discuss through this review. A PEM cell showing exemplary initial performance due to a high OER electrocatalyst activity that also has a high degradation rate will become obsolete before the targeted operational hours are met [79,82–85]. In this case, frequently replacing the electrocatalyst (and associated components) is expensive from an operational/capital expenditure perspective – reducing overall productivity due to downtime [85,86]. To further highlight the stability challenge in PEM electrolysers, an anode electrocatalyst made of RuO_2, with a Faradaic selectivity of 99.999999 % for the OER, will still dissolve at ~0.43 mg cm ^{2} annually (see the **Supplementary Information**). Electrocatalyst degradation is also an accumulative process, and the large operational hours in a PEM-WE (compared to applied durations in academic literature) will lead to a notable change in the electrocatalyst's activity and degradation of the MEA.

2.2. The electrocatalyst's properties should be transferable into a PEM-WE

Integrating an OER electrocatalyst into a PEM cell must not adversely alter the properties that gave its initially promising performance in the half cell. In this case, a material used for the most fundamental studies – a single-crystal (i.e., a thin layer of epitaxy-grown surface) – is not easily or as readily applicable to an industrial electrolyser as a polycrystalline

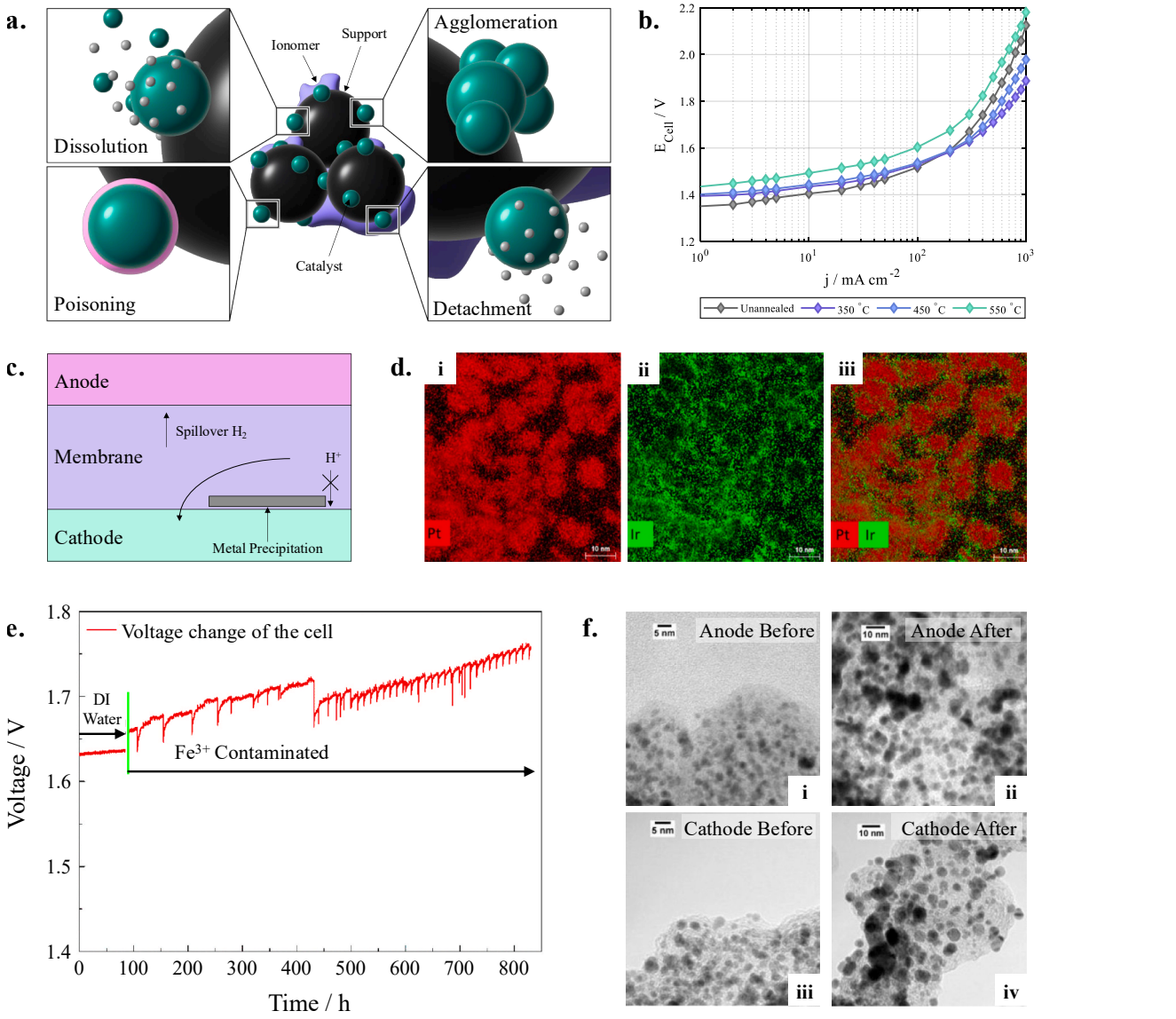

Fig. 2. **(a)** Potential degradation mechanisms of the electrocatalyst in an MEA. **(b)** PEM electrolyser performance of RuO_2 annealed at different temperatures [98]. **(c)** Metal deposition within the membrane, related H_2 spill over and increase in the system's resistance. **d)** SEM-EDX mapping of cathode catalyst near membrane (i) Pt map, (ii) Ir map, and (iii) overlay of Pt and Ir map [136]. **(e)** The impact of Fe^{3+} contamination on the cell performance [137]. **(f)** TEM of (i) fresh anodic catalyst (ii) used anode (iii) fresh cathode (iv) used cathode [138].

electrocatalyst, even if it has an outstanding utilisation factor (activity, durability, and cost). Analogously, many polycrystalline electrocatalyst screening studies use traditional synthesis methods (sol-gel, molten salt, Pechini method *etc.*) [31,87–92], with which scale-up offers its own challenges. Thus, while these approaches provide valuable insights into catalyst development using a half cell, their impact/influence on commercial PEM-WE performance is not yet fully understood [68,93].

Once the electrocatalyst is incorporated into a PEM cell, additional factors become important. As PEM electrolysers must operate at a high current density to minimise the levelized cost of H_2 (cost to produce 1 kg of H_2, including the estimated costs of capital investment required and the cost of operating the assets involved in its production) [94,95], the ohmic losses in the electrocatalytic layers (in addition to that in the membrane, PTLs, and bi-polar plates) are required to be as low as possible. This factor is often not considered when electrocatalysts are studied in half cells, where current densities are at least two orders of magnitude lower than in a PEM cell. Furthermore, the electrocatalytic layers in half cells (often drop cast layers on flat substrates) are often much thinner than the electrocatalytic layers found in a PEM cell (~10 μm), where a low contact resistance between the electrocatalyst particles becomes significant [96,97]. For instance, Xing et al. found that while RuO_2 with poor crystallinity showed superior performance below 200 mA cm^{-2} when compared to more crystalline samples, the latter showed better performance in PEM cells at higher current densities due to a lower film resistance (Fig. 2b) [98].

3. Key challenges for OER electrocatalysts in PEM water electrolysers

3.1. Electrocatalyst stability is a major challenge

The OER in a PEM-WE occurs at low pH and at potentials more positive than the standard oxidation potential of all metals (>1.5 V vs RHE) [99], meaning that pure metals are thermodynamically predicted to transition into oxides or ions [100,101]. These conditions thus favour catalyst dissolution [17,102–105], dopant leaching [106], structural and compositional modifications (Fig. 2a) [25,59,60,82,107–111]. While RuO_2 may be the most active OER catalyst, based on Pourbaix's data, Schalenbach et al. showed that Ir-, Pt-, and Rh-oxides are the only compounds thermodynamically stable for the OER up to 1.6 V vs RHE [100]. RuO_2 can be partially stabilised by mixing with other elements such as Ta, Sn, Nb etc. (see Section 5) [112–115]. However, this decreases the overall PEM cell performance [1,88,112] in part as these mixed oxides exhibit lower conductivity compared to metallic IrO_2 or RuO_2 [116–118].

As elegantly summarised by Roy et al. [51], RuO_2 corrosion (and ultimately Ru dissolution) under OER relevant potentials proceeds via the reaction: $RuO_2 + 2H_2O \rightarrow RuO_{4(aq)} + 4H^+ + 4e^-$, with its Faradaic selectivity reliant on the catalyst's physicochemical properties (mediated by the synthesis method), and operating conditions [16,119,120]. However, mechanistic details relating to individual steps of Ru dissolution, and their dependence on RuO_2 surface orientation and structure, remain convoluted. A point of focus, and debate, is whether the OER induces Ru dissolution and whether its activity correlates with the Ru dissolution rate (i.e. is there an inverse relationship between activity and stability) – as is believed to be the case. Recent theoretical work has shown that water oxidation and the OER induce the dissolution of the catalytically active Ru_{cus} sites by a preceding surface reconstruction, coupled with a loss of OER activity [121,122]. The dissolution rates of these Ru_{cus} sites [51–53] on pristine and defective (step, terraced or kinked, etc.) surfaces have been found to correlate, albeit to different extents, with the OER activity; These two processes are believed to share common reaction intermediates that can even mediate the OER pathway (i.e. are highly active for specific steps along the OER) and minimise its overpotential [119,123]. Further, dissolution may be stabilised by the water oxidation process and through the lattice oxygen evolution pathway [123]. Interestingly, however, recent experimental evidence hints that OER activity and dissolution-driven instability may not be correlated in this material – laying claim to the possibility that these two processes are decoupled, with important benefits in terms of electrocatalyst development for commercial applications [51]. Development of computational simulations and their pragmatic application [11], along with the development of experimental tools (e.g. synchrotron spectroscopies [124,125]) and growing accessibility to high-quality epitaxial films [126,127] will provide clarity on these important matters.

3.2. Corrosion alters the electrocatalyst's structure and activity

As previous sections imply, during prolonged operation in the anode's corrosive environment, the electrocatalyst undergoes amorphisation, phase segregation, and even complete dissolution – altering its morphology, surface topology and electronic properties, etc. (Fig. 2a) [128]. In particular, as many OER electrocatalysts are based on unique micro-/nano-structured architectures, they are particularly susceptible to particle growth and sintering, reducing the active surface area during operation (Fig. 2f) [25,80,81,129–131]. Dissolution and sintering issues can be accelerated at high current densities due to hot spot formation (i.e. localised areas with increased temperature), which can further damage the membrane, cascading the issues [132]. While these factors are important in a PEM cell under prolonged operation, the lower current densities and shorter timeframes typically used in half cell studies may not uncover or even initiate stability issues (Section 6). Corrosion-induced changes can even be beneficial for the activity when tested in half cells [133–135].

3.3. Corrosion leads to additional "non"-electrocatalytic changes in PEM-WE systems

In addition to corrosion-induced changes to the electrocatalyst, its instability adversely affects the properties of the catalytic layer (catalyst-ionomer) and membrane in a PEM-WE. For example, dissolution of RuO_2 can lead to the precipitation of Ru in the membrane (Fig. 2c), reducing conductivity to H^+ and thus increasing the high-frequency resistance [98]. Similar changes were seen in Ir-based anodes (Fig. 2d) [6,136,139], where leached cations block ion exchange sites in the membrane and ionomer [140]. Inazumi et al. [141], for example, studied the long-term stability of PEM-WEs and found that cell voltage increase was due to accumulation of Fe, Ni and Cr ions in the membrane (originating from the stainless steel tubing) [142]. The commonly used Nafion membrane and ionomer are especially vulnerable as metal ions, except Li^+, have a higher affinity towards Nafion's sulfonic groups compared to protons [143]. Substitution of a proton by metal ions can also impact water transport in the membrane due to bulkier solvated ions ($[M(H_2O)_x]^{y+}$ compared to H_3O^+) [144–146]. Even a small concentration of ions could be detrimental to PEM performance – for example, Li et al. observed that 1 ppm Fe^{3+} contamination immediately increased the cell voltage, and the degradation rate increased from 5.2 to 128.9 μV h^{-1} at 0.5 A cm^{-2} (Fig. 2e) [137]. The cations can also catalyse the Fenton reaction, promoting the formation of radicals like $HO^{\bullet}$, $HOO^{\bullet}$ and $H^{\bullet}$, which may damage the membrane and other components [147–151].

The cathode electrocatalyst (often Pt on carbon support) can also be influenced ('poisoned') by the dissolution of the anode materials [73,80,81,87,137,150,152–154]. Metal cations with a reduction potential higher than the operating potential of the cathode can be reduced, blocking the electrocatalytic surface and increasing the HER overpotential [155]. Metal cations that have more negative reduction potentials (e.g. Ca^{2+}, Ti^{4+}) do not deposit on the electrocatalyst but instead precipitate in the form of hydroxides or oxides at the membrane-cathode interface, increasing the resistivity of the MEA and decreasing the cell performance [156,157].

As highlighted in Sections 3.1-3.**3**; the instability of the

electrocatalyst not only influences its inherent ability to drive the OER but can also impact the membrane and cathode in a PEM cell. While reducing the cost of the electrocatalytic material is important for a PEM-WE, balancing this against the operating efficiency and stack lifetime is essential from an economic perspective. Thus, beyond research focusing on developing the electrocatalyst alone, dynamic changes and their influence on the stability of the new electrocatalyst when integrated into the MEA are areas requiring attention from the academic community [70]. This is all discussed further in the context of the electrocatalyst and operating conditions in Sections 4 and 5.

4. Preparation, characterisation, and performance of Ru-based OER electrocatalysts

4.1. A summary of literature performance, use of baseline materials and reproducibility

Ru-based electrocatalysts have been prepared in many ways to 'engineer' their properties (i.e. crystal structure, stoichiometry, atomic and structural defect presence, electrochemically active surface area (ECSA)) [158,159]. Often, however, attributes that improve activity are detrimental to long-term stability. For instance, a rough surface with a high ECSA, atomically defective surfaces [160,161] or amorphous materials show higher activity than a crystalline, stoichiometric benchmark but show poor stability against corrosion [18,102,162–166]. While these engineered electrocatalysts are commonly more active than the baseline (Fig. 3a and b, discussed below), their overpotential remains ~200 mV – seemingly confirming a theoretical limit as suggested by others [167].

Fig. 3a shows a comparison of electrocatalyst overpotentials reported in literature (summarised in **Appendix 2**) – green circles represent the engineered materials, and grey circles are baseline materials used for comparison. The scatter in the engineered and benchmark materials is similar – this suggests that a standard benchmark may not have been identified and makes comparison across the community innately biased. Similar order of magnitude differences in the observed activity of Ir and IrO_2 baseline materials have also been reported [168]. This is generally unsurprising, as a minor change in the synthesis procedure can change the material's physicochemical properties and observed OER activity (discussed in Section 5.2). For instance, we prepared a benchmark RuO_2 (via the fairly simple Adams Fusion method) [169] that showed an overpotential of ~200 mV – close to some of the best-performing electrocatalysts (Fig. SI1). Even when RuO_2 is prepared in such a trivial way, the performance metrics can vary (expanded on in Section 6) [159,170,171]. Trasatti, over 30 years ago [115], highlighted that two different operators in the same laboratory might not achieve similar electrochemical properties for, albeit more complex IrO_2–RuO_2 coated anodes, despite following identical preparation protocols (Fig. 3c). The voltametric charge varied depending on the solvent used and the operator conducting the experiment. Other studies also highlight disparities in voltametric charge of electrodes of alike compositions prepared in different laboratories [172]. A recent report from Tesch et al. [173] has shown that the OER overpotential of an electrocatalyst

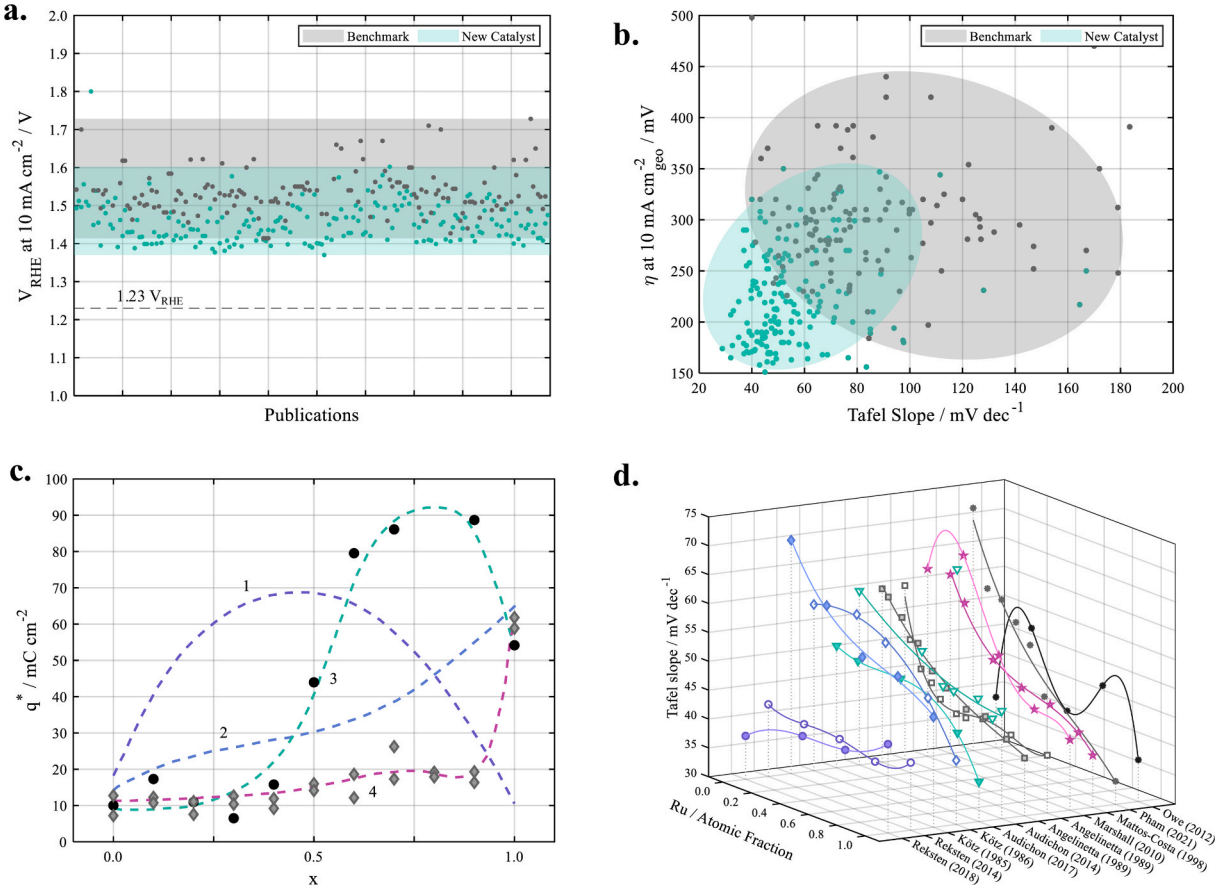

Fig. 3. (a) Overpotential of electrocatalysts reported in the literature (data from Appendix 2). The green circles are the engineered electrocatalyst, and the grey circles are the benchmark materials used for comparison. **(b)** The relationship between Tafel slope and overpotential. **(c)** Voltametric charge as a function of $xIrO_2+(1-x)RuO_2$ electrode for (1) precursors dissolved in water, (2) precursor dissolved in isopropanol, same operator, (3) precursor dissolved in water, another operator, (4) precursors in isopropanol another operator (figure and associated text in this caption were reproduced from the work of Trasatti) [115]. **(d)** Tafel slope of IrO_2–RuO_2 as a function of Ru content in literature (**Appendix 3**). (For interpretation of the references to colour in this figure legend, the reader is referred to the Web version of this article.)

depends on the experimenter, also for an experimenter themselves it can change based on pre-conditioning.

To highlight that composition alone is not an ideal descriptor of electrocatalytic behaviour, we show in Fig. 3d variations in the Tafel slope of $Ir_{1-x}Ru_xO_2$ prepared in different research groups (**Appendix 3**). While we can see a general decrease in the Tafel slope with an increase in the atomic fraction of Ru, the absolute values can vary significantly between two materials of similar composition. This extends to activity and stability – as we will highlight throughout Section 4 [21,28,38,44,174–177]. The difference in observed performance of similar materials also results from engineering aspects of the electrocatalytic layer, testing protocols, dynamic changes, etc., as we elaborate on in Section 5. Unless we are aided by standardised development protocols, the root cause of failure (or enhancement of the activity/stability) cannot be efficiently understood [178,179]. Through the following (sub-)sections, we will build on the topic of discrepancies in the performance of engineered and benchmark electrocatalysts.

4.2. Challenges with the synthesis of electrocatalysts

4.2.1. Bulk Ru-based electrocatalysts

Most Ru-based oxide electrocatalysts in literature are prepared using sol-gel synthesis, Pechini method, polyol synthesis, aqueous hydrolysis, molten salt method, co-precipitation, etc., involving oxidation of metal salt in a supporting matrix. The industry commonly uses the Adams-fusion method [31,87–92]. However, due to the innate complexity of the oxide synthesis process, achieving reproducible activity/stability data becomes an issue at the electrocatalyst development stage, leading to discrepancies noted in the earlier sections. The fabricated metal oxides' chemical/structural properties depend on the thermodynamic stability of phases, energetics of intermediates and products and kinetics of the process. Their properties can also differ based on the precursors used [180], diffusion of salts and their solubility, along with oxygen partial pressure [57,112,181,182]. Differences in decomposition kinetics among precursors and the oxide (facet) formation energy contribute also to surface/bulk ion segregation (Section 4.3). Achieving reproducible, scalable synthesis is particularly challenging when the material takes on unique micro-/nano-architectures (e.g. cubes, rods, fibres or wires), as it needs rigorous control over synthetic parameters [55,183–185]. Absolute transparency in reporting synthesis methods should be offered within publications to aid reproducibility. Nonetheless, these materials are being tested in PEM cells, as discussed in later sections.

4.2.2. Supported Ru-based electrocatalysts

Producing core-shell structures or dispersing nanoparticles (and single atoms) [186–188] on support materials (e.g., TiO_2 and SnO_2) [189,190], similar to how Pt is dispersed on a carbon support in the cathode, is a promising way to improve catalyst utilisation [182,191–193]. There are synthetic challenges in preparing core-shell or supported materials, where a broad range of species can result, such as single atom (atomic substitution in general), single site (a cluster that has one active site) and stand-alone (electrically isolated) RuO_2 nanoparticles [89,194,195]. With single-atom catalysts (SAC) a key synthetic challenge is maximising at.% loading while preventing the atoms from migrating and agglomerating (i.e. maintaining structural integrity) [186,187].

Due to a variety of particles in the ensemble, decoupling contributions from each component remains a challenge in this form. And while various supported materials were tested in PEM cells [90,196–199], this strategy is not yet ready for implementation. A key problem in the use of support materials (which are poorly conductive and inactive for the OER) is the lack of, or further loss of, conductivity from the ensemble due to oxidation or dissolution of ions. A decrease in the conductivity increases ohmic losses, especially at higher currents [7,200]. This is evidenced in several examples; In the case of an IrO_x/ATO (antimony tin-oxide) anode, the doped ions can leach out during operation [201], leading to a change in the conductivity and hence Ohmic losses, as observed by a 90 mV cell voltage increase of a PEM-WE at 1 A cm^{-2} after only 4 h of polarisation [190]. In the case of IrO_x supported on ATO, a Faradaic efficiency of only 94% for the OER was achieved due to the significant instability of the ATO support [202]. Higher anodic currents also inevitably result in the oxidation of the support during long operation, as observed in the case of micro-sized Ti metal particles [7] and Magnéli phase Ti suboxides Ti_nO_{2n-1} [203]. Detachment of the electrocatalyst particles from the support is another common problem in the absence of a strong metal-support interaction [202,204]. These challenges are also discussed from the context of the substrate in Section 5.4.

4.3. Bulk composition is not necessarily the surface composition

Even under meticulous control of growth and synthesis parameters, the (sub-)surface region of micro-/nano-particles can be different from the bulk [205–207]. This is particularly the case in bimetallic alloys and mixed-metal oxides, where factors governing surface (anti-)segregation were studied by Nørskov et al., via an understanding of the surface energy of transition metals (including Ru and Ir) [208].

Let us briefly look at empirical studies relating to Ru–Ir oxides as an example. When mixed oxides were synthesised by the annealing of an $Ir_{0.5}Ru_{0.5}$ alloy, the high temperatures led to a change in the surface composition from an Ru:Ir ratio of 1:1 to mainly being composed of Ir cations - a concentration gradient formed through the first few atomic layers (Fig. 4c and d) [209]. Owe et al. found that irrespective of the $Ir_xRu_{1-x}O_2$ composition, the surface Ir concentration was higher compared to the bulk [210]. A similar enrichment of Sn on the surface is reported in RuO_2–SnO_2 mixed oxides [211], and preferential segregation of Ir on the surface has also been reported in RuO_2–SnO_2–IrO_2 [114], IrO_2/SnO_2[212] etc. However, Nguyen observed surface dominance of Ru ions when $Ir_{0.5}Ru_{0.5}O_2$ was synthesised using a one-step or two-step synthesis [213]. Upon reviewing research that details the bulk and surface compositions of $Ir_{1-x}Ru_xO_2$, it is generally observed that Ir is more prevalent on the surface than in the bulk (Fig. 4b). The degree of phase segregation can vary based on the synthetic conditions resulting in considerable differences in the particle surface, particularly across studies [210,212,214]. Often the surface composition is estimated by XPS, and the bulk composition is determined by EDX or nominal composition. Considering the probing depth of XPS is a few unit cells [215], discrepancies in the sub-surface atomic layers may be more pronounced, and care should be taken to determine the correct values.

4.4. Electrocatalyst evolution during operation, activity improvement and stabilisation strategies

Key questions in the development of new electrocatalysts for the OER is to what extent the composition changes during operation, especially at higher currents and during long operation hours. And, if it changes, will the electrocatalyst maintain its performance for time periods relevant to industrial applications? Also, if the as-made electrocatalyst comprises a diverse number of active sites that are constantly changing, can one understand the origin of its improved performance or the root cause of failure, as mentioned in Section 4.1?

The (sub-)surface region of RuO_2 undergoes transformations in its physicochemical properties once it contacts the reaction medium [205–207,219]. This was seen, for example, in RuO_2 nanoparticles via changes in the Ru–O coordination number and bond length by in-situ x-ray absorption spectroscopy (XAS) (Fig. 5a–c) [216]. Of course, this region further changes when an electrical potential is applied [107,109,110,220,221]. As we have now discussed in earlier sections, RuO_2 is thermodynamically unstable at potentials driving the OER (>1.4 V), making its dissolution via changes in the valence state of Ru and Ru–O coordination number (forming RuO_x, $x > 2$ species) an inevitable, kinetically controlled process [16,216,222,223]. Using *in-situ* ambient

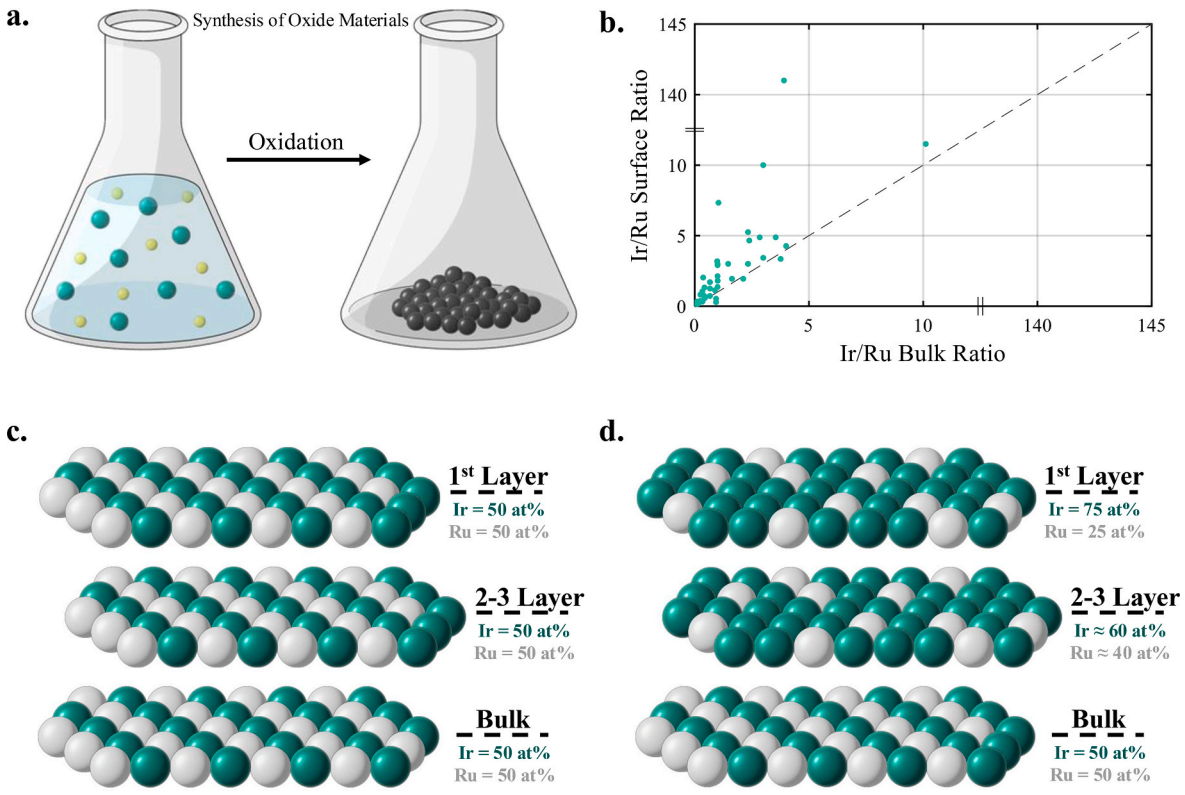

Fig. 4. Influences of annealing on the surface and sub-surface regions of Ir–Ru alloys. **(a)** Common synthesis methods for metal-oxides. **(b)** Comparing surface to bulk Ir/Ru ratios in literature (**Appendix 4**). Surface, sub-surface and bulk composition comparison for an as-made sputtered IrRu alloy **(c)** and of an $IrRuO_x$ catalyst after annealing **(d)** [209].

pressure XPS, Saveleva et al. show that RuO_2 undergoes a substantial potential-dependent transformation into other Ru species – even at potentials of 1.0 V, volatile Ru(VIII) species are detected, whose leaching results in an altered surface morphology [224]. Interestingly, the onset potential of the OER on RuO_2 coincides with its thermodynamic dissolution (Fig. 5d) [16], and various transient dissolution features are observed when oxygen atoms are inserted or removed from the oxides. To maintain charge neutrality in the electrocatalyst, either there will be a change in the valance state of Ru or a loss of lattice oxygen leading to the formation of an amorphous surface layer after a sufficient time (Fig. 5e) [217]. Studies have also suggested that partially oxidised or low valance state RuO_2 improves OER activity [225–229]. Since PEM-WEs are operated at high anodic currents, partially oxidised materials are likely to oxidise further after hours of operation. Thus, Ru metal or low valance state Ru catalysts will eventually form high valent Ru species during the OER [104]. Relating to the following text, we have tabulated (in Appendix 2) the Ru-based research work showing the leaching of at least one component.

Attempts have been made to improve the activity and stability of RuO_2 by doping with noble- and transition metals [14,230]. Select noble metals (e.g. Ir) are favoured as they preserve the surface functionality of RuO_2 for electrocatalytic reactions – this functionality is suspected to be rooted in its electronic and magnetic structure (determined by a very complex interplay of lattice-, spin-rotational, and time-reversal symmetries), as described in theoretical and experimental studies [117, 231–234]. The noble metals are also more stable against dissolution than other 3-5d transition metals in the acidic conditions within a PEM electrolyser; however, they are also more expensive than these elements, which motivates studies involving the latter. In either case, unless a solid solution is formed, there will be multiple phases in the particle [31,112, 211,235], with different physicochemical properties [236]. In particular, the metallic conductivity of RuO_2 will be hampered by changes in the electronic structure or by the formation of grain and domain boundaries. Of relevance for the potential application of RuO_2 in PEM cells is the use of Ti, Ir, Ta, Nb and particularly Ir as it offers stability while not compromising conductivity [112,209,237–239]. Danilovic et al. showed that when a near-perfect solid solution of an Ir–Ru alloy was subject to anodic polarisation, the atomic composition of the surface region altered, creating an Ir-rich environment after the leaching of the less stable Ru [209]. Cherevko et al. showed that $Ir_{1-x}Ru_xO_2$ nanoparticles had an Ir-enriched surface after the initial dissolution of Ru during OER [240]. In IrO_2–RuO_2 anodes, a disparity in the dissolution rates of constituent metal atoms was also observed [241]. Escudero-Escribano et al. showed that sputtering of sub-monolayer IrO_x layers onto a 40 nm RuO_2 thin film could drastically improve its stability, but as expected, the OER overpotential increased by 40 mV at 5 mA cm^{-2} [242]. Mayrhofer et al. found that the $IrRuO_x$ with 25 at.% Ir has a similar activity to that of RuO_2 initially. If the electrode is polarised with just 1 mA cm^{-2} for 5 min, the activity decreases drastically due to Ir enrichment (and Ru dissolution) on the surface and becomes closer to that of the initial activity of 60 at.% Ir (Fig. 6b) [241]. Similarly, the activity of the Au–Ru electrocatalyst changed significantly during cycling where the Tafel slope changed from 60 to 110 mV dec^{-1} after repeated cycling [243].

Walton et al. prepared doped RuO_2 using the significantly cheaper than noble metal Mg, Ni, Cu and Zn transition metals. The doped materials showed inferior performance to RuO_2, with dopant dissolution leaving a Ru-rich surface [63]. Tan et al. reported that Co-doped RuO_2 prepared via oxidation of a Co–Ru alloy undergoes significant leaching of Co metal during cyclic voltammetry between 1.2 and 1.5 V [244]. The cycling process increased the Ru oxidation state and changed the coordination environment around both the Co and Ru atoms. Ko et al. found that Ni K-edge XANES features of a $RuNiO_2$, even at open circuit voltage, are substantially different compared to the as-made material [245]. Ru and Ni leached into the solution during cyclic voltammetry with a higher rate of leaching for Ni during the first cycle. The electronic and local

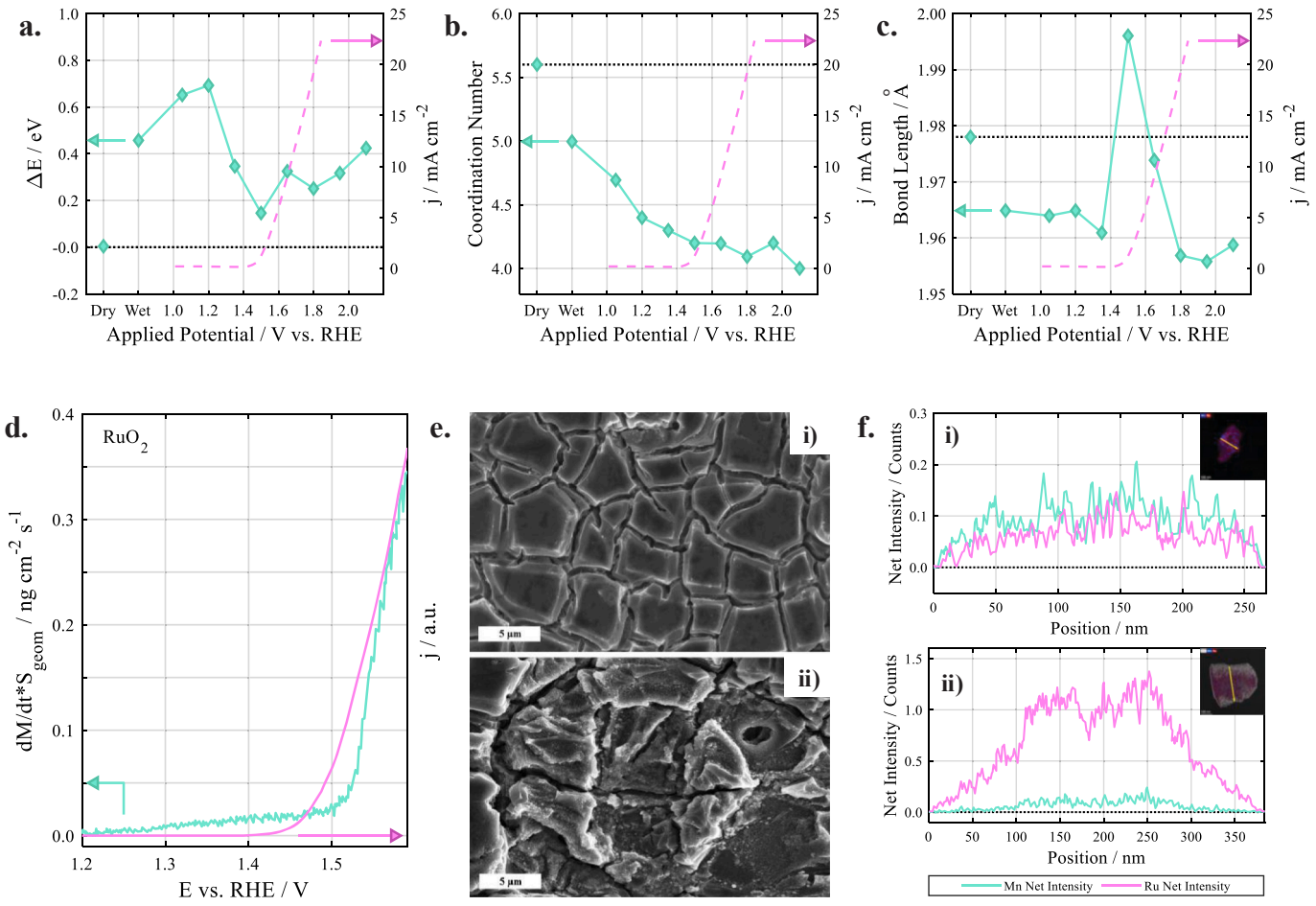

Fig. 5. In-situ investigation on RuO_2 nanoparticles in $0.5H_2SO_4$ electrolyte: **(a)** Potential-dependent edge energy shift relative to the dry (as-made) sample. **(b)** Potential-dependent Ru–O first shell coordination number. **(c)** Potential-dependent bond length for first shell Ru–O [216]. **(d)** Polarisation curve (blue line) and mass-spectra (red line) for RuO_2 electrode at 1 mV/s, in 0.5 M H_2SO_4 [16]. **(e)** RuO_2 DSA electrode before (i) and after (ii) OER for 1 h [217]. **(f)** Element distribution (from TEM) in RuMn electrode before (i) and after (ii) cyclic voltammetry [218]. (For interpretation of the references to colour in this figure legend, the reader is referred to the Web version of this article.)

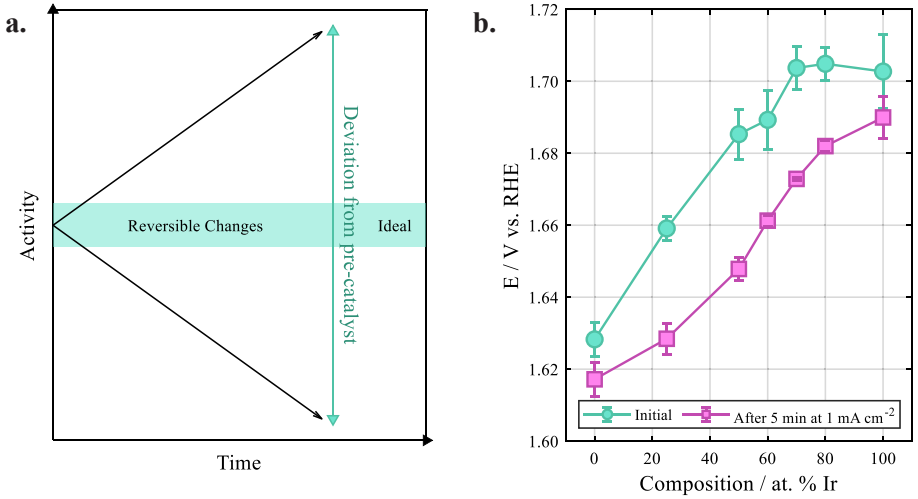

Fig. 6. **(a)** Structural evolution of a catalyst and change in activity with time – 'pre-catalyst' in the figure refers to the as-prepared material. **(b)** Variation of potential at a current density of 5 mA cm^{-2} in IrO_2–RuO_2 anodes before and after 5 min anodic polarisation at 1 mA cm^{-2} [241].

structure of $NiRuO_x$ became similar to hydrous RuO_x even at a low potential. Zhang et al. observed that Ru-M (M = Cr, Co or Zn) alloys undergo severe degradation during the OER, whereas Ru–Mn alloys form an amorphous layer of RuO_x that serves as a catalytically active component (Fig. 5f). Mn was not detected in the surface and sub-surface regions after electrochemical cycling [218]. The leaching of Mn and

subsequent formation of vacant sites on the Ir–Ru-rich oxide surface was also seen in an Ir–Ru–Mn 'nano-cactus' during an operational cycle [246]. Dissolution of Sr and a change in the composition and morphology were also found in a SrIrRu alloy tested for the OER, concurrent with a decrease in stability [247]. Using relatively robust $Ru_{1-x}Mn_xO_2$ DSA electrodes, we observed that while these electrodes show lower overpotential at 10 mA cm ^{2} (Fig. SI2) after 24 h of electrolysis, more than 80 % of Mn leached into the solution. Leaching of Ru also increased significantly.

While the majority of the above-described Ru-based OER electrocatalysts consist of rutile RuO_2, the perovskite (ABO_3) and pyrochlore ($A_2B_2O_7$) are also touted as promising structures to reduce the noble metal content of applied materials as they offer elemental composition tunability by the interchange of ions at the A and B sites [21,22,40,42–44]. However, they are not yet viable alternatives for electrocatalysts in PEM cells. In Ru-based perovskites, the leaching of elements from the cationic sites during the OER changes the surface composition into amorphous RuO_x with low concentrations of other ions [39]. While it was proposed based on theoretical studies that $SrRuO_3$ should show good OER performance [12], Kim et al. found that the activity of $SrRuO_3$ perovskite nanoparticles decayed during anodic polarisation [248]. In this instance, ICP-OES showed that elemental leaching resulted in a final Ru/Sr ratio of 0.16. Ji et al. [249] found that both Sr and Ru leach into the electrolyte and showed the absence of Sr cations at the surface of the electrode after 30 h of OER at 10 mA cm ^{2}. Concerning pyrochlores, the extent of A-site and B-site dissolution varies across the literature; in some studies, more than 50% dissolution of A-sites was reported [21,38,44,175–177], whereas other studies claimed no dissolution [250]. Hubert et al. indicated, using different A site elements (A = Y, Nd, Gd, Bi), that ions losses from pyrochlores during the OER as well as their degree of dissolution differ based on the element itself. After the dissolution of the A-sites, these materials again form oxidised, electrocatalytically active RuO_x-species [39,44].

In terms of SACs, continued development is needed in terms of stability [251–255]. Efforts were made to minimise Ru dissolution [252–256] using a variety of supports, including Pt_3–Cu alloy, Co–N4, Co_3O_4, CoFe and NiFe double layer hydroxides and nitrogen-carbon network (Ru–N4) [251–257]. Of note, Li et al. and Zhai et al. have shown Ru SACs to drive the OER at 200 mA cm ^{2} ($\eta = 1.5$ V) and 100 mA cm ^{2} ($\eta = 1.54$ V), respectively, with stability claimed for over 100 h [251,257].

4.5. Deconvoluting the intrinsic activity of a constantly changing electrocatalyst in an ensemble measurement

Despite reports of higher activities in engineered Ru-based materials against a baseline material [63,258], their long-term stability under industrial conditions remains questionable. Overwhelming evidence exists of structural reconstruction, dissolution of the host and leaching of dopants (**Appendix 2**) – all of which can change the reaction kinetics and thermodynamics [101,107,108,110,259–262]. Overall there is a lack of clarity regarding the "true" catalyst composition and factors that govern its performance. As eluded to the introduction, the question remains on what should be assigned as the actual activity or root cause of instability - a specific property or a convolution of many aspects [109].

Answering such a question is not trivial from an experimental and theoretical perspective. A small fraction of the catalyst can account for more or less of the observed turnover [263]. For instance, to highlight the complexity of this issue: The degree of water dissociation, intermediate state binding energies and overall activity/stability trends, were shown to depend strongly on the lattice orientation and bonding environment around an active site in RuO_2 [11,51–53]. Even minor changes in the material's surface quality influence the specific capacitance and thus the ECSA, affecting the observed performance [264]. However, reported electrocatalytic data is most commonly a macroscopic property – an averaged behaviour of the ensemble encompassing a variety of structural features and a superimposition of different reactions [265,266]. This is logical considering the geometry of currently used half cells and that synthesis methods result in a wide distribution of particle sizes of innate heterogeneity; as implied above, different lattice planes and topological features within (edges, steps, kinks, etc.) have distinct chemical affinity, activation energy and reactivity for steps along the OER [267–271]. They also give a spatially nonuniform current or potential distribution. Thus, the same material can have a non-negligible contrast in performance when tested in different laboratories [258,272]. These observations, and the differences in baseline material performance, once again indicate that standard characterisation methods for OER electrocatalysts, such as those reported for solar cells and other energy storage devices, are needed [273–276].

5. The electrocatalytic layer and testing protocols

5.1. Electrocatalytic layer preparation

To evaluate the performance in a PEM-WE, an electrode is prepared by casting the catalyst on a conductive substrate using a polymer-based binder (ionomer), sometimes with a support material or additive to promote particle-to-particle contact. The porosity, agglomerate size, and ionomer distribution of this heterogeneous layer facilitate proton transport from the membrane, electrons transfer to the current collector, and reactant interaction with the active sites (Fig. 7a). Thus, when the electrocatalyst is tested in a PEM cell, it is unsurprising that its observed performance differs due to various other factors; electrode coating process, the electrolyte type, testing procedure (conditioning protocol, acquisition method) and dynamic changes of the catalytic layer (e.g. degradation and bubble formation) [67,168,277–285].

Commonly used coating methods (e.g. drop casting, spray- or dip-coating) result in a distribution of electrocatalyst (electrical conductor) and ionomer (proton conductor) that may not be uniform, with the further presence of cracks or formation of isolated catalyst pockets producing electrically disconnected paths (Fig. 7a). These cracks can disrupt the continuous electron transfer path, reducing the catalyst layers electronic conductivity [286]. Proton transport, relying on the continuity of the ionomer network, can be hindered by the presence of cracks [287]. The structural attributes of the CL, such as the distribution of ionomers, can directly influence proton transport. The ionic conductivity of this binder is orders of magnitude lower than the electrical conductivity of the catalyst, varying based on thickness, temperature and applied potential [288]. Thus, when an external potential is applied to the substrate, the potential distribution across the catalytic layer varies. For H_2 production to progress efficiently, the electrocatalyst particles must be seamlessly connected to both the proton and electron transport pathways. The catalytic sites lacking access to either will remain inactive and unutilised. In addition, recent studies have found that binders such as Nafion ionomer, and PTFE, conventionally viewed as inert, can interact with catalysts leading to substantial alteration in their activities [284,289].

5.2. Considerations regarding mass loading of the electrocatalyst

At the half cell stage (where much of the fundamental catalyst development happens), figures of merit are mainly reported in terms of the overpotential at 10 mA cm_{geo}^{2} (c.f. 'geo' is the geometric surface area of the electrode), the change in this overpotential after 2 hr^{290} or through a mass normalised activity. We find however that there is no consistent value in the literature for the electrocatalyst's mass loading in a given geometric area (as seen from the summary plot in Fig. 7c) – despite a strong dependence of the overpotential at a given current density on this mass loading parameter (seen in Fig. 7b and b **inset**), highlighting the need for a standardised practice in the evaluation of electrocatalyst loading [161,291,292]. However, as geometric area and mass normalised activities are engineering perspectives of an electrode,

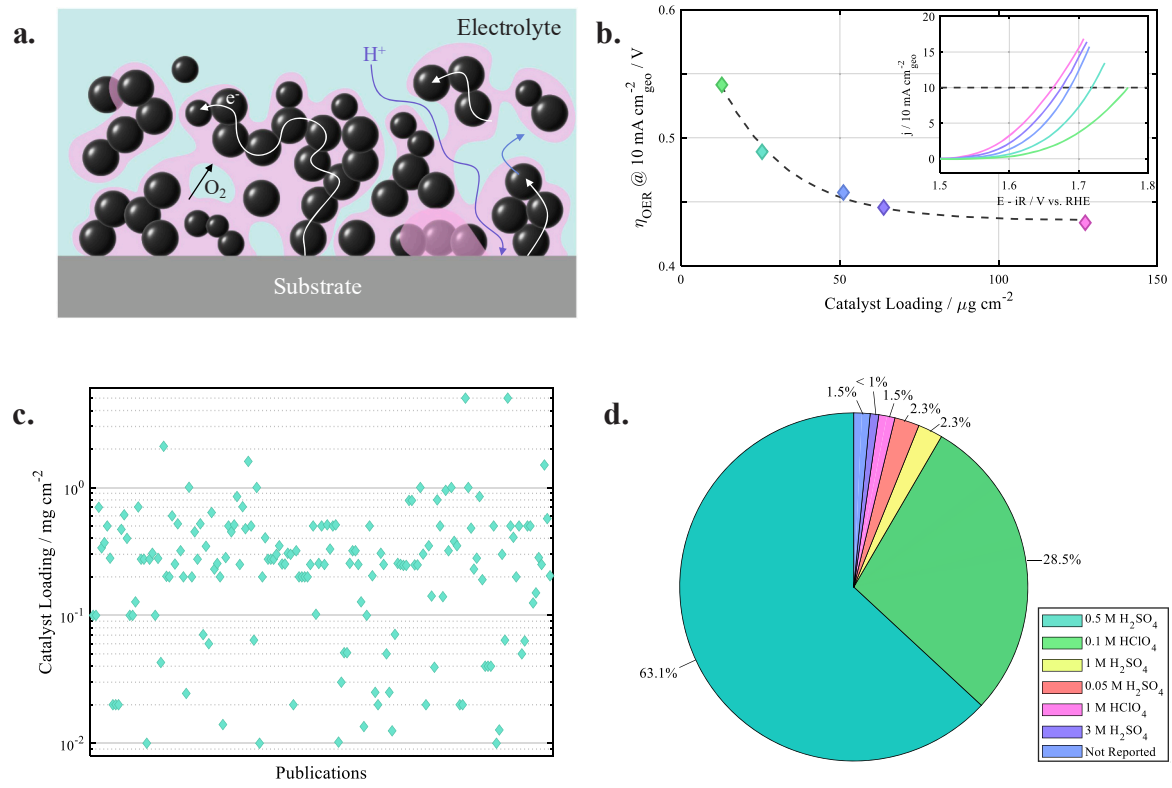

Fig. 7. (a) Nonuniformity and conductivity challenges in a catalytic layer. (b) OER overpotential at 10 mA cm^{-} [2] using IrO_2 NPs (nanoparticles, ≈7 nm diameter) as a function of electrocatalyst loading [291] (c) Catalytic loading used in literature (Appendix 1). (d) Electrolytes used in the literature (Appendix 1).

they do not always reflect variations in the catalyst's intrinsic activity stemming also from a physicochemical property. In this regard, an important aspect to further consider is normalisation against the ECSA. The importance of this point was highlighted by McCrory et al. [293] concerning the standardisation of OER electrocatalyst testing protocols in general and more specifically with respect to RuO_2 by Reiser et al. [264] – this latter study provided an upper limit of specific capacitance for use in determining the ECSA of geometrically ill-defined RuO_2 catalysts from their double-layer capacitance.

5.3. Electrolyte

While 0.5 M H_2SO_4 and 0.1 M $HClO_4$ were common electrolyte choices in literature, our investigation revealed that a diverse range of other electrolytes being used (as summarised in Fig. 7d).The choice of supporting electrolyte can also alter the observed activity. For example, Sunde et al. found that the electrolyte could substantially change the OER rate in acidic media, and a higher OER rate is observed with more electronegative anions [278]. Similarly, Arminio-Ravelo et al. found that the Ir based electrocatalysts are less active in H_2SO_4 compared to $HClO_4$, likely due to stronger adsorption of SO_4^{2} ions compared to ClO_4 ions [277]. In contrast, Alia et al. [168] found that polycrystalline Ir and IrO_x nanoparticles demonstrate little to no difference in their OER activities in 0.1 M $HClO_4$ and 0.5H_2SO_4.

5.4. Electrode substrate

As we described in Section 4.2, and briefly bring the communities attention to again here, the electrode substrate used to immobilise the electrocatalytic particles plays a role in the electrochemical response [199,283]. To highlight an example, Geiger et al. saw that the stability and activity of Ir-black depended on the backing substrate. The electrocatalyst's initial activity on gold or glassy carbon (GC) is higher than on boron-doped diamond (BDD) and fluorine-doped tin oxide (FTO). This was attributed to higher contact resistance between BDD and FTO substrates and the electrocatalyst. In a long-term galvanostatic study, the electrocatalyst showed a more abrupt increase in overpotential on GC and FTO compared to gold and BDD. These observations related to passivation (surface oxidation) of the GC and dissolution of FTO – it did not represent the behaviour of the pristine electrocatalyst. Clearly, an electrocatalyst on two different supports can show different electrochemical responses, and one should be particularly aware that passivation or degradation of the substrate can result in an incorrect estimation of the electrocatalyst's activity or stability.

6. State of art evolution of the electrocatalyst

Several protocols [272,290,294–296] have been reported for evaluating OER electrocatalysts. Among these, the protocol reported by McCrory et al. [290] is commonly adopted. This protocol recommends key performance metrics for OER catalysts, including the overpotential required to achieve a current density of 10 mA cm ^{2} (geometric area) and stability of this overpotential over a 2-h duration [290]. However, a review of the material-centric literature reveals a notable gap in properly reporting the catalytic activity properties of the materials.

6.1. The Tafel slope dilemma

As discussed in relation to transition state theory by Exner and Over [297,298], the OER mechanism in the low overpotential region (η = 0.2–0.3 V) starts from a different RuO_2 surface structure than in the higher overpotential region (η > 0.3 V), resulting in contrasting Tafel slope values. In systems with a complex micro-/nanostructure, this variation can be from 40 to 200 mV dec ^{1} in different potential regions, demonstrated using a model RuO_2 DSA electrode (Fig. 8a). There are often two orders of magnitude differences between current densities

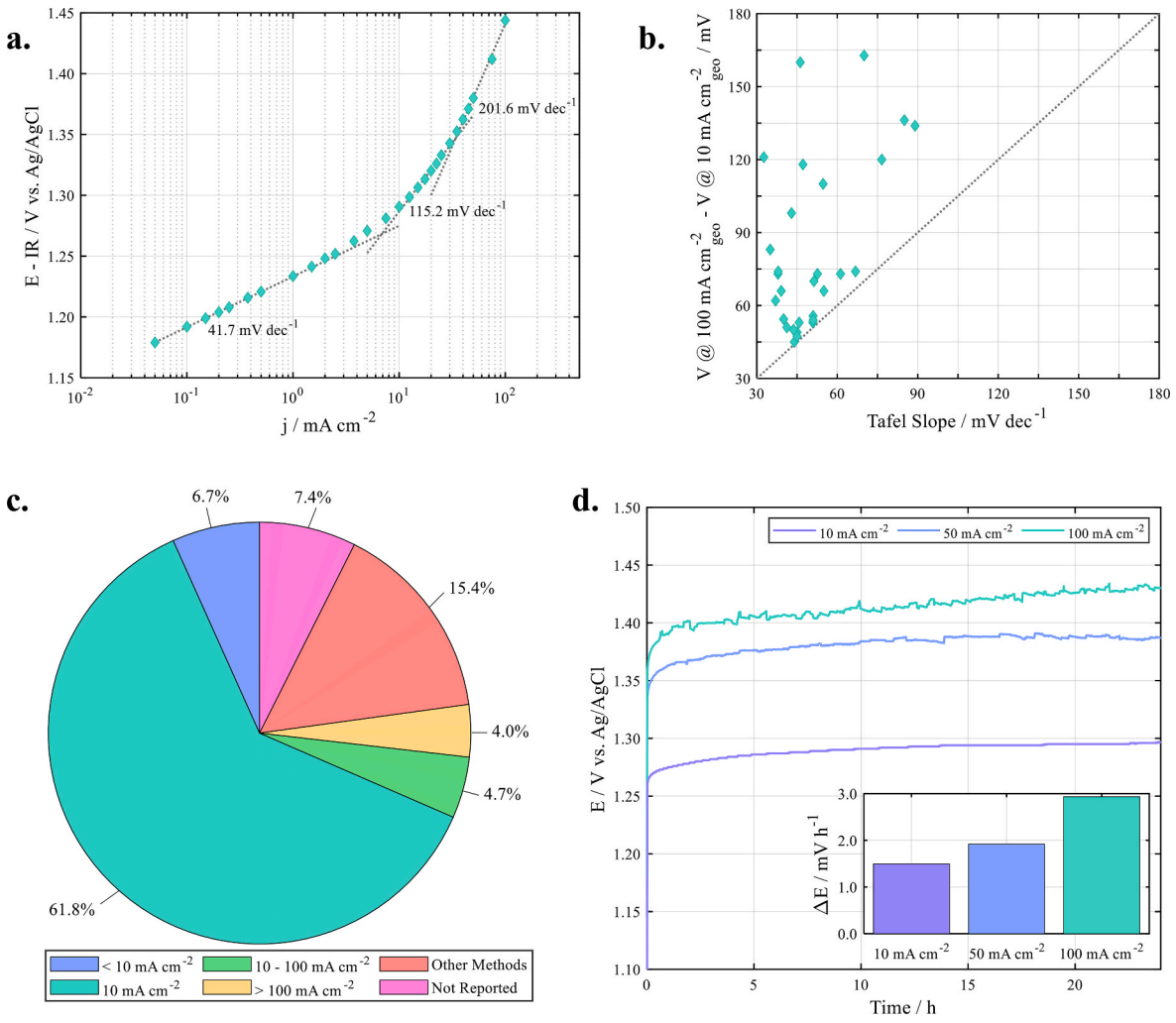

Fig. 8. **(a)** Polarisation curve of RuO_2 DSA electrode in 0.5 M H_2SO_4, highlighting three Tafel regions between 0.1 mA cm^{-} [2] to 100 mA cm^{-} [2]. **(b)** The difference in overpotential at 100 mA cm^{-} [2] and 10 mA cm^{-} [2] in randomly selected papers in the literature (Table SI1). **(c)** Stability studies parameters reported in the literature. **(d)** Stability assessment of RuO_2 DSA-electrode at different current densities.

used to study model catalysts and those used in an applied scenario. However, most articles report only one Tafel slope (typically in low overpotential regions); consequently, the overpotential required to achieve 100 mA cm ^{2} or 1 mA cm ^{2} does not always scale with the reported Tafel slope [28,292,299,300]. Through a study of the Tafel slope and difference between potentials at 10 mA cm ^{2} and 100 mA cm ^{2} in 30 randomly selected reports cited in this review, we can indeed highlight that the activity data at higher currents indeed do not scale with the Tafel slope (Fig. 8b, papers from Table SI1). In recent articles, the Tafel slope is sometimes estimated by less than a decade of the current density range, which may result in an erroneous representation of electrocatalytic performance (also clear from Fig. 7a). As we noted earlier, sometimes the catalyst that performs well at lower currents fails to do so at higher currents – this has been further demonstrated using three model electrocatalysts (Fig. SI4) and a 20 % RuO_2/ATO electrocatalyst (Fig. 9). RuO_2/ATO showed a low overpotential at lower

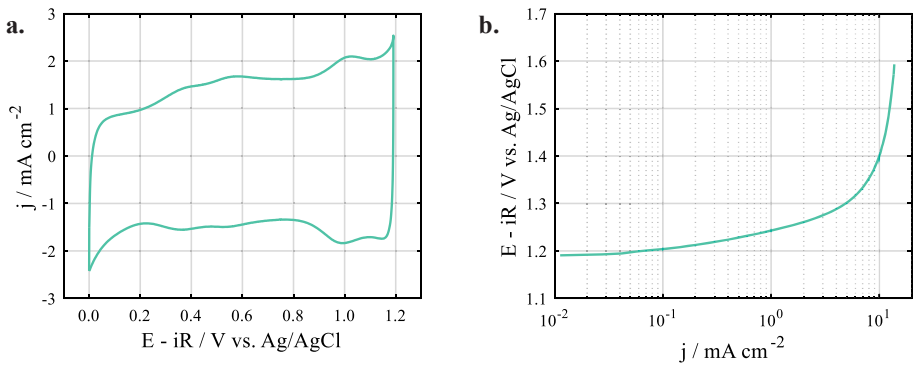

Fig. 9. Oxygen evolution studies on 20% RuO_2 supported onto antimony doped tin oxide in 0.5 M H_2SO_4 electrolyte. **(a)** Cyclic voltammetry of the electrode shows a fingerprint consistent with RuO_2. **(b)** Linear sweep voltammetry of the electrode. The electrode demonstrates about 210 mV overpotential to reach 10 mA cm^{-2}.

currents yet struggled to achieve a higher current density. This suggests that the reporting of Tafel slopes in higher potential regions would also be very useful. However, this is overall a complex topic and reporting should be done with clear descriptions of testing protocols.

6.2. Stability at low vs. high current densities

As stated in Section 5.2, we find that the majority of literature articles report stability as a change in overpotential at 10 mA cm ^{2} or show chronoamperometry at a fixed overpotential for a number of hours (this has been summarised in Fig. 8c) [290]. Less than 10 % report stability at currents over 10 mA cm ^{2}. The significance of this can be seen in a few example: Zhang et al. found that an Ru–Mn alloy-derived electrocatalyst only saw a 100 mV increase in overpotential after 720 h at 10 mA cm ^{2}, however, at 100 mA cm ^{2}, the overpotential increased instantly (by more than 210 mV in less than 1 h) [218]. RuO_2 nanosheets showed stability at 1 mA cm ^{2}, but at 10 mA cm ^{2} the overpotential increased from 260 mV to 520 mV after 6 h. We found similar observations using RuO_2 DSAs at low and high currents (Fig. 8d).

As we alluded to in earlier sections, the continuous dissolution of elements and reconstruction of the surface can also generate a higher ECSA, masking under limited testing times, a change in overpotential. For example, we found that a $RuMnO_2$ electrode had an increase in ECSA after 24 h OER testing at 10 mA cm ^{2} (Fig. SI3). If the catalyst loading is high, the degradation of the catalyst can be masked due to the sluggish dissolution of the active component, even in a PEM cell [281,301]. If the stability test was performed for a long duration (O_{100h}), a false conclusion of a low degradation rate (high stability) may be drawn. Thus, galvanostatic or potentiostatic stability tests should be supplemented with measurement of dissolved ions in the electrolyte [302].

7. Perspectives and summary

Developments in the field of Ru-based electrocatalysts have reduced the OER overpotential to low values (<200 mV) at 10 mA cm ^{2} (Fig. 3a). Given that theoretical studies from Koper et al. [167] suggest that a surface will always possess an intrinsic overpotential, it may be that the OER activity has reached a lower limit, nonetheless, the stability of these electrocatalysts at industry-relevant current density values remains an issue. Fabricating progressively more complex materials and reporting their OER performance under non-standardised testing conditions seems to hinder progress toward the development of a stable electrocatalyst for PEM systems. An inherent heterogeneity in the electrocatalysts stemming from commonly used synthesis methods complicates our ability to gain fundamental insights. Single-crystals (offering the highest degree of structural/compositional sensitivity) allow one to develop an understanding of structure-activity/stability relationships – a cogent (and increasingly recognised) approach to the design of an active catalyst in its polycrystalline form. In this latter case, synthetic methods for catalysts with a controlled size distribution, shape or composition are required to go from single crystal to industrially relevant powder volumes, all the while preserving the positive physical attributes identified in the former stage. However, various traits of a polycrystalline electrocatalyst overlap in their contribution to its OER performance, underscoring the necessity for investigations employing multiple operando techniques, ideally in the same electrochemical cell at the single crystal level. It is also essential to conduct round-robin three-electrode testing of commercially available OER electrocatalysts across diverse laboratory environments, such as those attempted for fuel cells [303], and electrolysers [304–306]. The advantage of round-robin tests is to provide a full picture of the applicability of a measurement protocol and to determine possible weak points. We suggest that intra-lab- *vs.* inter-lab-uncertainty in the activity of OER catalysts must be recognised and accounted for when comparing results from different research groups. Beyond achieving an understanding of changes in properties at the nanoscale (and how they may be controlled), it is crucial to examine how this knowledge can be applied and transferred from the half-cell level into a PEM-WE – a necessary step in translating lab-scale knowledge into an applied setting. This will also include method development to understand issues not encountered in a three-electrode half-cell, such as bubble problems and catalyst heterogeneity.

In principle, for industrial applications, understanding the insights of catalytic materials beyond what is achieved in the preceding phases is not overly critical if the synthesis method can be scaled and the material can provide stable and economical operation. To this end, there is a need to accelerate the testing of catalysts with promising stability at a lab scale under more industrially relevant current densities and to standardise the testing protocols (below). The latter, as discussed, will enable fairer comparison between reported data. Since a commercial PEM electrolyser works at high current densities (1–2 A cm ^{2}, 1.4–2.5 V at a catalyst loading of 2–5 mg cm ^{2}) for time periods 50–80 ($\times$ 1000) hr, the stability and activity tests at 10 mA cm ^{2} for relatively short timescales limit our ability to assess a materials readiness for applied settings. To compare activities at low current ranges, instead of reporting the overpotential at 10 mA cm ^{2}, it may be useful to report mass and ECSA normalised activity at a fixed overpotential; 300 mV (approximately the typical OER onset for IrO_2) is a reasonable point. The long-term stability of a catalyst may be gauged at higher current densities as 10 mA cm ^{2} is too low when compared to the target practical ones of 1 A cm ^{2} or more for at least 100 h – with an emphasis on analysis of catalyst degradation, used catalyst composition, and stoichiometry. We note that applied catalysts will need to operate by 2030 under gradually higher standards: 3 A cm ^{2} using less than 1.8 V for >80 ($\times$ 1000) hr with loadings of 0.2–0.4 mg cm ^{2} within the MEA. Notably, they will be expected to have degradation rates of ~2–2.3 mV kh ^{1} (0.13 % khr ^{1}).

CRediT authorship contribution statement

Shailendra K. Sharma: Writing – review & editing, Writing – original draft, Formal analysis, Data curation, Conceptualization. **Chang Wu:** Writing – review & editing, Formal analysis, Data curation. **Niall Malone:** Writing – review & editing, Writing – original draft, Data curation. **Laura J. Titheridge:** Writing – review & editing, Visualization, Resources, Formal analysis. **Chuan Zhao:** Writing – review & editing. **Prasanth Gupta:** Writing – review & editing, Investigation, Data curation. **Hicham Idriss:** Writing – review & editing, Investigation, Formal analysis. **John V. Kennedy:** Writing – review & editing, Funding acquisition. **Vedran Jovic:** Writing – review & editing, Writing – original draft, Supervision, Funding acquisition, Formal analysis, Conceptualization. **Aaron T. Marshall:** Writing – review & editing, Writing – original draft, Supervision, Funding acquisition, Formal analysis, Conceptualization.

Declaration of competing interest

The authors declare that they have no known competing financial interests or personal relationships that could have appeared to influence the work reported in this paper.

Acknowledgements

The authors thank Dr. Simon K. Moser for helpful discussions. Funding support was provided by the New Zealand Ministry of Business, Innovation and Employment (MBIE) Grant number: C05X2004.

References

[1] Carmo M, Fritz DL, Mergel J, Stolten D. A comprehensive review on PEM water electrolysis. Int J Hydrogen Energy 2013;38(12):4901–34. https://doi.org/10.1016/j.ijhydene.2013.01.151.

[2] Shiva Kumar S, Himabindu V. Hydrogen production by PEM water electrolysis – a review. Mater. Sci. Energy Technol. 2019;2(3):442–54. https://doi.org/10.1016/j.mset.2019.03.002.

[3] Grigoriev SA, Fateev VN, Bessarabov DG, Millet P. Current status, research trends, and challenges in water electrolysis science and technology. Int J Hydrogen Energy 2020;45(49):26036–58. https://doi.org/10.1016/j.ijhydene.2020.03.109.

[4] Lamy C, Millet P. A critical review on the definitions used to calculate the energy efficiency coefficients of water electrolysis cells working under near ambient temperature conditions. J Power Sources 2020;447:227350. https://doi.org/10.1016/j.jpowsour.2019.227350.

[5] Millet P, Mbemba N, Grigoriev SA, Fateev VN, Aukauloo A, Etiévant C. Electrochemical performances of PEM water electrolysis cells and perspectives. Int J Hydrogen Energy 2011;36(6):4134–42. https://doi.org/10.1016/j.ijhydene.2010.06.105.

[6] Lettenmeier P, Wang R, Abouatallah R, Helmly S, Morawietz T, Hiesgen R, Kolb S, Burggraf F, Kallo J, Gago AS, et al. Durable Membrane Electrode Assemblies for proton exchange membrane electrolyzer systems operating at high current densities. Electrochim Acta 2016;210:502–11. https://doi.org/10.1016/j.electacta.2016.04.164.

[7] Rozain C, Mayousse E, Guillet N, Millet P. Influence of iridium oxide loadings on the performance of PEM water electrolysis cells: Part II – advanced oxygen electrodes. Appl Catal B Environ 2016;182:123–31. https://doi.org/10.1016/j.apcatb.2015.09.011.

[8] Kibsgaard J, Chorkendorff I. Considerations for the scaling-up of water splitting catalysts. Nat Energy 2019;4(6):430–3. https://doi.org/10.1038/s41560-019-0407-1.

[9] Parry SJ. Abundance and distribution of palladium, platinum, iridium and gold in some oxide minerals. Chem Geol 1984;43(1):115–25. https://doi.org/10.1016/0009-2541(84)90142-6.

[10] Minke C, Suermann M, Bensmann B, Hanke-Rauschenbach R. Is iridium demand a potential bottleneck in the realization of large-scale PEM water electrolysis? Int J Hydrogen Energy 2021;46(46):23581–90. https://doi.org/10.1016/j.ijhydene.2021.04.174.

[11] Over H. Fundamental studies of planar single-crystalline oxide model electrodes (RuO_2, IrO_2) for acidic water splitting. ACS Catal 2021;11(14):8848–71. https://doi.org/10.1021/acscatal.1c01973.

[12] Man IC, Su H-Y, Calle-Vallejo F, Hansen HA, Martínez JI, Inoglu NG, Kitchin J, Jaramillo TF, Nørskov JK, Rossmeisl J. Universality in oxygen evolution electrocatalysis on oxide surfaces. ChemCatChem 2011;3(7):1159–65. https://doi.org/10.1002/cctc.201000397.

[13] Yu J, He Q, Yang G, Zhou W, Shao Z, Ni M. Recent advances and prospective in ruthenium-based materials for electrochemical water splitting. ACS Catal 2019;9(11):9973–10011. https://doi.org/10.1021/acscatal.9b02457.

[14] Sun H, Jung W. Recent advances in doped ruthenium oxides as high-efficiency electrocatalysts for the oxygen evolution reaction. J Mater Chem A 2021;9(28):15506–21. https://doi.org/10.1039/D1TA03452A. 10.1039/D1TA03452A.

[15] Song S, Zhang H, Ma X, Shao Z, Baker RT, Yi B. Electrochemical investigation of electrocatalysts for the oxygen evolution reaction in PEM water electrolyzers. Int J Hydrogen Energy 2008;33(19):4955–61. https://doi.org/10.1016/j.ijhydene.2008.06.039.

[16] Cherevko S, Geiger S, Kasian O, Kulyk N, Grote J-P, Savan A, Shrestha BR, Merzlikin S, Breitbach B, Ludwig A, et al. Oxygen and hydrogen evolution reactions on Ru, RuO_2, Ir, and IrO_2 thin film electrodes in acidic and alkaline electrolytes: a comparative study on activity and stability. Catal Today 2016;262:170–80. https://doi.org/10.1016/j.cattod.2015.08.014.

[17] Danilovic N, Subbaraman R, Chang K-C, Chang SH, Kang YJ, Snyder J, Paulikas AP, Strmcnik D, Kim Y-T, Myers D, et al. Activity–stability trends for the oxygen evolution reaction on monometallic oxides in acidic environments. J Phys Chem Lett 2014;5(14):2474–8. https://doi.org/10.1021/jz501061n.

[18] Kim JY, Choi J, Kim HY, Hwang E, Kim H-J, Ahn SH, Kim S-K. Activity and stability of the oxygen evolution reaction on electrodeposited Ru and its thermal oxides. Appl Surf Sci 2015;359:227–35. https://doi.org/10.1016/j.apsusc.2015.10.082.

[19] Weininger JL, Russell RR. Corrosion of the ruthenium oxide catalyst at the anode of a solid polymer electrolyte cell. J Electrochem Soc 1978;125(9):1482–6. https://doi.org/10.1149/1.2131700.

[20] Kim M, Park J, Kang M, Kim JY, Lee SW. Toward efficient electrocatalytic oxygen evolution: emerging opportunities with metallic pyrochlore oxides for electrocatalysts and conductive supports. ACS Cent Sci 2020;6(6):880–91. https://doi.org/10.1021/acscentsci.0c00479.

[21] Kim J, Shih P-C, Tsao K-C, Pan Y-T, Yin X, Sun C-J, Yang H. High-performance pyrochlore-type yttrium ruthenate electrocatalyst for oxygen evolution reaction in acidic media. J Am Chem Soc 2017;139(34):12076–83. https://doi.org/10.1021/jacs.7b06808.

[22] Horowitz HS, Longo JM, Horowitz HH. Oxygen electrocatalysis on some oxide pyrochlores. J Electrochem Soc 1983;130(9):1851–9. https://doi.org/10.1149/1.2120111.

[23] Wang C, Jin L, Shang H, Xu H, Shiraishi Y, Du Y. Advances in engineering RuO_2 electrocatalysts towards oxygen evolution reaction. Chin Chem Lett 2021;32(7):2108–16. https://doi.org/10.1016/j.cclet.2020.11.051.

[24] Zhou F, Zhang L, Li J, Wang Q, Chen Y, Chen H, Lu G, Chen G, Jin H, Wang S, et al. Novel engineering of ruthenium-based electrocatalysts for acidic water oxidation: a mini review. Eng. Rep. 2021;3(8):e12437. https://doi.org/10.1002/eng2.12437.

[25] Spöri C, Kwan JTH, Bonakdarpour A, Wilkinson DP, Strasser P. The stability challenges of oxygen evolving catalysts: towards a common fundamental understanding and mitigation of catalyst degradation. Angew Chem Int Ed 2017;56(22):5994–6021. https://doi.org/10.1002/anie.201608601.

[26] Zhang L, Jang H, Liu H, Kim MG, Yang D, Liu S, Liu X, Cho J. Sodium-Decorated Amorphous/Crystalline RuO2 with Rich Oxygen Vacancies: a pobust pH-universal oxygen evolution electrocatalyst. Angew Chem Int Ed 2021;60(34):18821–9. https://doi.org/10.1002/anie.202106631.

[27] Tian Y, Wang S, Velasco E, Yang Y, Cao L, Zhang L, Li X, Lin Y, Zhang Q, Chen L. A Co-doped nanorod-like RuO_2 electrocatalyst with abundant oxygen vacancies for acidic water oxidation. iScience 2020;23(1):100756. https://doi.org/10.1016/j.isci.2019.100756.

[28] Chen S, Huang H, Jiang P, Yang K, Diao J, Gong S, Liu S, Huang M, Wang H, Chen Q. Mn-doped RuO_2 nanocrystals as highly active electrocatalysts for enhanced oxygen evolution in acidic media. ACS Catal 2020;10(2):1152–60. https://doi.org/10.1021/acscatal.9b04922.

[29] Lin Y, Tian Z, Zhang L, Ma J, Jiang Z, Deibert BJ, Ge R, Chen L. Chromium-ruthenium oxide solid solution electrocatalyst for highly efficient oxygen evolution reaction in acidic media. Nat Commun 2019;10(1):162. https://doi.org/10.1038/s41467-018-08144-3.

[30] Forgie R, Bugosh G, Neyerlin KC, Liu Z, Strasser P. Bimetallic Ru electrocatalysts for the oer and electrolytic water splitting in acidic media. Electrochem Solid State Lett 2010;13(4):B36. https://doi.org/10.1149/1.3290735.

[31] Jirkovský J, Makarova M, Krtil P. Particle size dependence of oxygen evolution reaction on nanocrystalline RuO_2 and $Ru_{0.8}Co_{0.2}O_{2-x}$. Electrochem Commun 2006;8(9):1417–22. https://doi.org/10.1016/j.elecom.2006.06.027.

[32] Neyerlin KC, Bugosh G, Forgie R, Liu Z, Strasser P. Combinatorial study of high-surface-area binary and ternary electrocatalysts for the oxygen evolution reaction. J Electrochem Soc 2009;156(3):B363. https://doi.org/10.1149/1.3049820.

[33] He J, Li W, Xu P, Sun J. Tuning electron correlations of RuO_2 by co-doping of Mo and Ce for boosting electrocatalytic water oxidation in acidic media. Appl Catal B Environ 2021;298:120528. https://doi.org/10.1016/j.apcatb.2021.120528.

[34] Wu Y, Tariq M, Zaman WQ, Sun W, Zhou Z, Yang J. Bimetallic doped RuO_2 with manganese and iron as electrocatalysts for favorable oxygen evolution reaction performance. ACS Omega 2020;5(13):7342–7. https://doi.org/10.1021/acsomega.9b04237.

[35] Wu Y, Tariq M, Zaman WQ, Sun W, Zhou Z, Yang J. Ni–Co codoped RuO_2 with outstanding oxygen evolution reaction performance. ACS Appl Energy Mater 2019;2(6):4105–10. https://doi.org/10.1021/acsaem.9b00266.

[36] Ping X, Liu Y, Chen S, Ran N, Zheng L, Wang M, Guo L, Wei Z. Tailoring B-site of lead-ruthenate pyrochlore for boosting acidic water oxidation activity and stability. Appl Catal B Environ 2022;318:121884. https://doi.org/10.1016/j.apcatb.2022.121884.

[37] Liu T, Yang S, Guan J, Niu J, Zhang Z, Wang F. Quenching as a route to defect-rich ru-pyrochlore electrocatalysts toward the oxygen evolution reaction. Small Methods 2022;6(1):2101156. https://doi.org/10.1002/smtd.202101156.

[38] Kim J, Shih P-C, Qin Y, Al-Bardan Z, Sun C-J, Yang H. A porous pyrochlore $Y_2[Ru_{1.6}Y_{0.4}]O_{7-\delta}$ electrocatalyst for enhanced performance towards the oxygen evolution Reaction in acidic media. Angew Chem Int Ed 2018;57(42):13877–81. https://doi.org/10.1002/anie.201808825.

[39] Hubert MA, Patel AM, Gallo A, Liu Y, Valle E, Ben-Naim M, Sanchez J, Sokaras D, Sinclair R, Nørskov JK, et al. Acidic oxygen evolution reaction activity–stability relationships in Ru-based pyrochlores. ACS Catal 2020;10(20):12182–96. https://doi.org/10.1021/acscatal.0c02252.

[40] Song HJ, Yoon H, Ju B, Kim D-W. Highly efficient perovskite-based electrocatalysts for water oxidation in acidic environments: a mini review. Adv Energy Mater 2021;11(27):2002428. https://doi.org/10.1002/aenm.202002428.

[41] Sardar K, Petrucco E, Hiley CI, Sharman JDB, Wells PP, Russell AE, Kashtiban RJ, Sloan J, Walton RI. Water-splitting electrocatalysis in acid conditions using ruthenate-iridate pyrochlores. Angew Chem Int Ed 2014;53(41):10960–4. https://doi.org/10.1002/anie.201406668. 2022/09/29.

[42] Feng Q, Zou J, Wang Y, Zhao Z, Williams MC, Li H, Wang H. Influence of surface oxygen vacancies and ruthenium valence state on the catalysis of pyrochlore oxides. ACS Appl Mater Interfaces 2020;12(4):4520–30. https://doi.org/10.1021/acsami.9b19352.

[43] Feng Q, Zhang Z, Huang H, Yao K, Fan J, Zeng L, Williams MC, Li H, Wang H. An effective strategy to tune the oxygen vacancy of pyrochlore oxides for electrochemical energy storage and conversion systems. Chem Eng J 2020;395:124428. https://doi.org/10.1016/j.cej.2020.124428.

[44] Kuznetsov DA, Naeem MA, Kumar PV, Abdala PM, Fedorov A, Müller CR. Tailoring lattice oxygen binding in ruthenium pyrochlores to enhance oxygen evolution activity. J Am Chem Soc 2020;142(17):7883–8. https://doi.org/10.1021/jacs.0c01135.

[45] Miao X, Zhang L, Wu L, Hu Z, Shi L, Zhou S. Quadruple perovskite ruthenate as a highly efficient catalyst for acidic water oxidation. Nat Commun 2019;10(1):3809. https://doi.org/10.1038/s41467-019-11789-3.

[46] Liu H, Wang Z, Li M, Zhao X, Duan X, Wang S, Tan G, Kuang Y, Sun X. Rare-earth-regulated Ru-O interaction within the pyrochlore ruthenate for electrocatalytic oxygen evolution in acidic media. Sci China Mater 2021;64(7):1653–61. https://doi.org/10.1007/s40843-020-1571-y.

[47] Zhang C, Wang F, Xiong B, Yang H. Regulating the electronic structures of mixed B-site pyrochlore to enhance the turnover frequency in water oxidation. Nano Converg 2022;9(1):22. https://doi.org/10.1186/s40580-022-00311-z.

[48] Wang L, Sofer Z, Pumera M. Will any crap we put into graphene increase its electrocatalytic effect? ACS Nano 2020;14(1):21–5. https://doi.org/10.1021/acsnano.9b00184.

[49] Stoerzinger KA, Qiao L, Biegalski MD, Shao-Horn Y. Orientation-dependent oxygen evolution activities of rutile IrO_2 and RuO_2. J Phys Chem Lett 2014;5(10):1636–41. https://doi.org/10.1021/jz500610u.

[50] Rao RR, Kolb MJ, Halck NB, Pedersen AF, Mehta A, You H, Stoerzinger KA, Feng Z, Hansen HA, Zhou H, et al. Towards identifying the active sites on RuO_2(110) in catalyzing oxygen evolution. Energy Environ Sci 2017;10(12):2626–37. https://doi.org/10.1039/C7EE02307C. 10.1039/C7EE02307C.

[51] Roy C, Rao RR, Stoerzinger KA, Hwang J, Rossmeisl J, Chorkendorff I, Shao-Horn Y, Stephens IEL. Trends in activity and dissolution on RuO_2 under oxygen evolution conditions: particles versus well-defined extended surfaces. ACS Energy Lett 2018;3(9):2045–51. https://doi.org/10.1021/acsenergylett.8b01178.

[52] Rao RR, Kolb MJ, Hwang J, Pedersen AF, Mehta A, You H, Stoerzinger KA, Feng Z, Zhou H, Bluhm H, et al. Surface orientation dependent water dissociation on rutile ruthenium dioxide. J Phys Chem C 2018;122(31):17802–11. https://doi.org/10.1021/acs.jpcc.8b04284.

[53] Rao RR, Kolb MJ, Giordano L, Pedersen AF, Katayama Y, Hwang J, Mehta A, You H, Lunger JR, Zhou H, et al. Operando identification of site-dependent water oxidation activity on ruthenium dioxide single-crystal surfaces. Nat Catal 2020;3(6):516–25. https://doi.org/10.1038/s41929-020-0457-6.

[54] Rao RR, Huang B, Katayama Y, Hwang J, Kawaguchi T, Lunger JR, Peng J, Zhang Y, Morinaga A, Zhou H, et al. pH- and cation-dependent water oxidation on rutile RuO_2(110). J Phys Chem C 2021;125(15):8195–207. https://doi.org/10.1021/acs.jpcc.1c00413.

[55] Feng Y-Y, Si S, Deng G, Xu Z-X, Pu Z, Hu H-S, Wang C-B. Copper-doped ruthenium oxide as highly efficient electrocatalysts for the evolution of oxygen in acidic media. J Alloys Compd 2022;892:162113. https://doi.org/10.1016/j.jallcom.2021.162113.

[56] Chapman PM, Guerra LM. The "So What?" factor. Mar Pollut Bull 2005;50(12):1457–8. https://doi.org/10.1016/j.marpolbul.2005.10.010.

[57] Akbashev AR. Electrocatalysis on oxide surfaces: fundamental challenges and opportunities. Curr Opin Electrochem 2022;35:101095. https://doi.org/10.1016/j.coelec.2022.101095.

[58] Akbashev AR. Electrocatalysis goes nuts. ACS Catal 2022;12(8):4296–301. https://doi.org/10.1021/acscatal.2c00123.

[59] Luo X, Tan X, Ji P, Chen L, Yu J, Mu S. Surface reconstruction-derived heterostructures for electrochemical water splitting. Inside Energy 2022:100091. https://doi.org/10.1016/j.enchem.2022.100091.

[60] Liu X, Meng J, Zhu J, Huang M, Wen B, Guo R, Mai L. Comprehensive understandings into complete reconstruction of precatalysts: synthesis, applications, and characterizations. Adv Mater 2021;33(32):2007344. https://doi.org/10.1002/adma.202007344. 2022/09/26.

[61] Ehelebe K, Escalera-López D, Cherevko S. Limitations of aqueous model systems in the stability assessment of electrocatalysts for oxygen reactions in fuel cell and electrolyzers. Curr Opin Electrochem 2021;29:100832. https://doi.org/10.1016/j.coelec.2021.100832.

[62] Cherevko S. Stability and dissolution of electrocatalysts: building the bridge between model and "real world" systems. Curr Opin Electrochem 2018;8:118–25. https://doi.org/10.1016/j.coelec.2018.03.034.

[63] Burnett DL, Petrucco E, Rigg KM, Zalitis CM, Lok JG, Kashtiban RJ, Lees MR, Sharman JDB, Walton RI. M,Ru)O2 (M = Mg, Zn, Cu, Ni, Co) Rutiles and their use as oxygen evolution electrocatalysts in membrane electrode assemblies under acidic conditions. Chem Mater 2020;32(14):6150–60. https://doi.org/10.1021/acs.chemmater.0c01884.

[64] Lazaridis T, Stühmeier BM, Gasteiger HA, El-Sayed HA. Capabilities and limitations of rotating disk electrodes versus membrane electrode assemblies in the investigation of electrocatalysts. Nat Catal 2022;5(5):363–73. https://doi.org/10.1038/s41929-022-00776-5.

[65] Knöppel J, Möckl M, Escalera-López D, Stojanovski K, Bierling M, Böhm T, Thiele S, Rzepka M, Cherevko S. On the limitations in assessing stability of oxygen evolution catalysts using aqueous model electrochemical cells. Nat Commun 2021;12(1):2231. https://doi.org/10.1038/s41467-021-22296-9.

[66] Lagadec MF, Grimaud A. Water electrolysers with closed and open electrochemical systems. Nat Mater 2020;19(11):1140–50. https://doi.org/10.1038/s41563-020-0788-3.

[67] Fathi Tovini M, Hartig-Weiß A, Gasteiger HA, El-Sayed HA. The discrepancy in oxygen evolution reaction catalyst lifetime explained: RDE vs MEA - dynamicity within the catalyst layer matters. J Electrochem Soc 2021;168(1):014512. https://doi.org/10.1149/1945-7111/abdcc9.

[68] Klingenhof M, Hauke P, Kroschel M, Wang X, Merzdorf T, Binninger C, Ngo Thanh T, Paul B, Teschner D, Schlögl R, et al. Anion-tuned layered double hydroxide anodes for anion exchange membrane water electrolyzers: from catalyst screening to single-cell performance. ACS Energy Lett 2022;7(10):3415–22. https://doi.org/10.1021/acsenergylett.2c01820.

[69] Alia SM, Ha M-A, Anderson GC, Ngo C, Pylypenko S, Larsen RE. The roles of oxide growth and sub-surface facets in oxygen evolution activity of iridium and its impact on electrolysis. J Electrochem Soc 2019;166(15):F1243. https://doi.org/10.1149/2.0771915jes.

[70] Alia SM. Current research in low temperature proton exchange membrane-based electrolysis and a necessary shift in focus. Curr Opin Chem Eng 2021;33:100703. https://doi.org/10.1016/j.coche.2021.100703.

[71] IRENA. In: *Green hydrogen cost reduction: Scaling up Electrolysers to Meet the 1.5°C climate goal*; abu dhabi; 2020. https://www.irena.org/-/media/Files/IRENA/Agency/Publication/2020/Dec/IRENA_Green_hydrogen_cost_2020.pdf.

[72] FCH-JU. In: Key performance indicators (KPIs) for FCH Research and Innovation, 2020-2030; 2020. p. 1–30. https://www.eera-fch.eu/news-and-resources/2121:the-jp-fch-kpis.html.

[73] Andolfatto F, Durand R, Michas A, Millet P, Stevens P. Solid polymer electrolyte water electrolysis: electrocatalysis and long-term stability. Int J Hydrogen Energy 1994;19(5):421–7. https://doi.org/10.1016/0360-3199(94)90018-3.

[74] Riedmayer R, Paren BA, Schofield L, Shao-Horn Y, Mallapragada D. Proton exchange membrane electrolysis performance targets for achieving 2050 expansion goals constrained by iridium supply. Energy Fuels 2023;37(12):8614–23. https://doi.org/10.1021/acs.energyfuels.3c01473.

[75] Krishnan S, Koning V, Theodorus de Groot M, de Groot A, Mendoza PG, Junginger M, Kramer GJ. Present and future cost of alkaline and PEM electrolyser stacks. Int J Hydrogen Energy 2023;48(83):32313–30. https://doi.org/10.1016/j.ijhydene.2023.05.031.

[76] Clapp M, Zalitis CM, Ryan M. Perspectives on current and future iridium demand and iridium oxide catalysts for PEM water electrolysis. Catal Today 2023;420:114140. https://doi.org/10.1016/j.cattod.2023.114140.

[77] Bareiß K, de la Rua C, Möckl M, Hamacher T. Life cycle assessment of hydrogen from proton exchange membrane water electrolysis in future energy systems. Appl Energy 2019;237:862–72. https://doi.org/10.1016/j.apenergy.2019.01.001.

[78] Colella WG, James BD, Moton JM, Saur G, Ramsden T. Techno-economic analysis of PEM electrolysis for hydrogen production. Electrolytic hydrogen production workshop, vol. 27. Golden, Colorado: NREL; 2014.

[79] Ayers K. The potential of proton exchange membrane–based electrolysis technology. Curr Opin Electrochem 2019;18:9–15. https://doi.org/10.1016/j.coelec.2019.08.008.

[80] Millet P, Ngameni R, Grigoriev SA, Mbemba N, Brisset F, Ranjbari A, Etiévant C. PEM water electrolyzers: from electrocatalysis to stack development. Int J Hydrogen Energy 2010;35(10):5043–52. https://doi.org/10.1016/j.ijhydene.2009.09.015.

[81] Siracusano S, Van Dijk N, Backhouse R, Merlo L, Baglio V, Aricò AS. Degradation issues of PEM electrolysis MEAs. Renew Energy 2018;123:52–7. https://doi.org/10.1016/j.renene.2018.02.024.

[82] Chen F-Y, Wu Z-Y, Adler Z, Wang H. Stability challenges of electrocatalytic oxygen evolution reaction: from mechanistic understanding to reactor design. Joule 2021;5(7):1704–31. https://doi.org/10.1016/j.joule.2021.05.005.

[83] Hubert MA, King LA, Jaramillo TF. Evaluating the case for reduced precious metal catalysts in proton exchange membrane electrolyzers. ACS Energy Lett 2022;7(1):17–23. https://doi.org/10.1021/acsenergylett.1c01869.

[84] Ayers KE, Anderson EB, Capuano C, Carter B, Dalton L, Hanlon G, Manco J, Niedzwiecki M. Research advances towards low cost, high efficiency PEM electrolysis. ECS Trans 2010;33(1):3–15. https://doi.org/10.1149/1.3484496.

[85] Babic U, Suermann M, Büchi FN, Gubler L, Schmidt TJ. Critical review—identifying critical gaps for polymer electrolyte water electrolysis development. J Electrochem Soc 2017;164(4):F387–99. https://doi.org/10.1149/2.1441704jes.

[86] Takenaka H, Torikai E, Kawami Y, Wakabayashi N. Solid polymer electrolyte water electrolysis. Int J Hydrogen Energy 1982;7(5):397–403. https://doi.org/10.1016/0360-3199(82)90050-7.

[87] Millet P, Andolfatto F, Durand R. Design and performance of a solid polymer electrolyte water electrolyzer. Int J Hydrogen Energy 1996;21(2):87–93. https://doi.org/10.1016/0360-3199(95)00005-4.

[88] Marshall A. Electrocatalysts for the oxygen evolution electrode in water electrolysers using proton exchange membranes: synthesis and characterisation. Trondheim: Norwegian University of Science and Technology; 2005.

[89] Haverkamp RG, Marshall AT, Cowie BCC. Energy resolved XPS depth profile of (IrO_2, RuO_2, Sb_2O_5, SnO_2) electrocatalyst powder to reveal core-shell nanoparticle structure. Surf Interface Anal 2011;43(5):847–55. https://doi.org/10.1002/sia.3644. 2022/09/24.

[90] Wu X, Scott K. RuO_2 supported on Sb-doped SnO_2 nanoparticles for polymer electrolyte membrane water electrolysers. Int J Hydrogen Energy 2011;36(10):5806–10. https://doi.org/10.1016/j.ijhydene.2010.10.098.

[91] Reksten A, Moradi F, Seland F, Sunde S. Iridium-ruthenium mixed oxides for oxygen evolution reaction prepared by pechini synthesis. ECS Trans 2014;58(25):39–50. https://doi.org/10.1149/05825.0039ecst.

[92] Siracusano S, Van Dijk N, Payne-Johnson E, Baglio V, Aricò AS. Nanosized IrO_x and $IrRuO_x$ electrocatalysts for the O_2 evolution reaction in PEM water electrolysers. Appl Catal B Environ 2015;164:488–95. https://doi.org/10.1016/j.apcatb.2014.09.005.

[93] Browne MP, Dodwell J, Novotny F, Jaśkaniec S, Shearing PR, Nicolosi V, Brett DJL, Pumera M. Oxygen evolution catalysts under proton exchange membrane conditions in a conventional three electrode cell vs. electrolyser device: a comparison study and a 3D-printed electrolyser for academic labs. J Mater Chem A 2021;9(14):9113–23. https://doi.org/10.1039/D1TA00633A. 10.1039/D1TA00633A.

[94] Villagra A, Millet P. An analysis of PEM water electrolysis cells operating at elevated current densities. Int J Hydrogen Energy 2019;44(20):9708–17. https://doi.org/10.1016/j.ijhydene.2018.11.179.

[95] Wang T, Cao X, Jiao L. PEM water electrolysis for hydrogen production: fundamentals, advances, and prospects. Carbon Neutra 2022;1(1):21. https://doi.org/10.1007/s43979-022-00022-8.

[96] Bernt M, Schramm C, Schröter J, Gebauer C, Byrknes J, Eickes C, Gasteiger HA. Effect of the IrO_x conductivity on the anode electrode/porous transport layer interfacial resistance in PEM water electrolyzers. J Electrochem Soc 2021;168(8): 084513. https://doi.org/10.1149/1945-7111/ac1eb4.

[97] Bernt M, Siebel A, Gasteiger HA. Analysis of voltage losses in pem water electrolyzers with low platinum group metal loadings. J Electrochem Soc 2018; 165(5):F305–14. https://doi.org/10.1149/2.0641805jes.

[98] Ma H, Liu C, Liao J, Su Y, Xue X, Xing W. Study of ruthenium oxide catalyst for electrocatalytic performance in oxygen evolution. J Mol Catal Chem 2006;247(1): 7–13. https://doi.org/10.1016/j.molcata.2005.11.013.

[99] Pourbaix M. Atlas of electrochemical equilibria in aqueous solutions. New York: Pergamon Press Oxford; 1966.

[100] Schalenbach M, Zeradjanin AR, Kasian O, Cherevko S, Mayrhofer KJ. A perspective on low-temperature water electrolysis–challenges in alkaline and acidic technology. Int J Electrochem Sci 2018;13(2):1173–226.

[101] Miles MH, Thomason MA. Periodic variations of overvoltages for water electrolysis in acid solutions from cyclic voltammetric studies. J Electrochem Soc 1976;123(10):1459. https://doi.org/10.1149/1.2132619.

[102] Reier T, Oezaslan M, Strasser P. Electrocatalytic oxygen evolution reaction (OER) on Ru, Ir, and Pt catalysts: a comparative study of nanoparticles and bulk materials. ACS Catal 2012;2(8):1765–72. https://doi.org/10.1021/cs3003098.

[103] Martelli GN, Ornelas R, Faita G. Deactivation mechanisms of oxygen evolving anodes at high current densities. Electrochim Acta 1994;39(11):1551–8. https://doi.org/10.1016/0013-4686(94)85134-4.

[104] Cherevko S, Zeradjanin AR, Topalov AA, Kulyk N, Katsounaros I, Mayrhofer KJJ. Dissolution of noble metals during oxygen evolution in acidic media. ChemCatChem 2014;6(8):2219–23. https://doi.org/10.1002/cctc.201402194. 2022/09/26.

[105] Siracusano S, Baglio V, Stassi A, Ornelas R, Antonucci V, Aricò AS. Investigation of IrO_2 electrocatalysts prepared by a sulfite-couplex route for the O_2 evolution reaction in solid polymer electrolyte water electrolyzers. Int J Hydrogen Energy 2011;36(13):7822–31. https://doi.org/10.1016/j.ijhydene.2010.12.080.

[106] Gu X-K, Camayang JCA, Samira S, Nikolla E. Oxygen evolution electrocatalysis using mixed metal oxides under acidic conditions: challenges and opportunities. J Catal 2020;388:130–40. https://doi.org/10.1016/j.jcat.2020.05.008.

[107] Gao R, Deng M, Yan Q, Fang Z, Li L, Shen H, Chen Z. Structural variations of metal oxide-based electrocatalysts for oxygen evolution reaction. Small Methods 2021;5 (12):2100834. https://doi.org/10.1002/smtd.202100834.

[108] Selvam NCS, Du L, Xia BY, Yoo PJ, You B. Reconstructed water oxidation electrocatalysts: the impact of surface dynamics on intrinsic activities. Adv Funct Mater 2021;31(12):2008190. https://doi.org/10.1002/adfm.202008190.

[109] Kou Z, Li X, Zhang L, Zang W, Gao X, Wang J. Dynamic surface chemistry of catalysts in oxygen evolution reaction. Small Sci 2021;1(7):2100011. https://doi.org/10.1002/smsc.202100011.

[110] Jiang H, He Q, Zhang Y, Song L. Structural self-reconstruction of catalysts in electrocatalysis. Accounts Chem Res 2018;51(11):2968–77. https://doi.org/10.1021/acs.accounts.8b00449.

[111] Li T, Kasian O, Cherevko S, Zhang S, Geiger S, Scheu C, Felfer P, Raabe D, Gault B, Mayrhofer KJJ. Atomic-scale insights into surface species of electrocatalysts in three dimensions. Nat Catal 2018;1(4):300–5. https://doi.org/10.1038/s41929-018-0043-3.

[112] Puthiyapura VK, Pasupathi S, Basu S, Wu X, Su H, Varagunapandiyan N, Pollet B, Scott K. $Ru_xNb_{1-x}O_2$ catalyst for the oxygen evolution reaction in proton exchange membrane water electrolysers. Int J Hydrogen Energy 2013;38(21): 8605–16. https://doi.org/10.1016/j.ijhydene.2013.04.100.

[113] Marshall AT, Sunde S, Tsypkin M, Tunold R. Performance of a PEM water electrolysis cell using $Ir_xRu_yTa_zO_2$ electrocatalysts for the oxygen evolution electrode. Int J Hydrogen Energy 2007;32(13):2320–4. https://doi.org/10.1016/j.ijhydene.2007.02.013.

[114] Hutchings R, Müller K, Kötz R, Stucki S. A structural investigation of stabilized oxygen evolution catalysts. J Mater Sci 1984;19(12):3987–94. https://doi.org/10.1007/BF00980762.

[115] Trasatti S. Physical electrochemistry of ceramic oxides. Electrochim Acta 1991;36 (2):225–41. https://doi.org/10.1016/0013-4686(91)85244-2.

[116] Jovic V, Koch RJ, Panda SK, Berger H, Bugnon P, Magrez A, Smith KE, Biermann S, Jozwiak C, Bostwick A, et al. Dirac nodal lines and flat-band surface state in the functional oxide RuO_2. Phys Rev B 2018;98(24):241101. https://doi.org/10.1103/PhysRevB.98.241101.

[117] Nelson JN, Ruf JP, Lee Y, Zeledon C, Kawasaki JK, Moser S, Jozwiak C, Rotenberg E, Bostwick A, Schlom DG, Shen K, Moreschini L. Dirac nodal lines protected against spin-orbit interaction in IrO_2. Phys Rev Mater 2019;3(6): 064205. https://doi.org/10.1103/PhysRevMaterials.3.064205.

[118] S. Trasatti, G. L. Properties of conductive transition metal oxides with rutile-type structure. In Electrodes of conductive metallic oxides Part A, Trasatti, S. Ed.; Elsevier scientific publishing company, pp 301-358.

[119] Kötz R, Stucki S, Scherson D, Kolb DM. In-situ identification of RuO_4 as the corrosion product during oxygen evolution on ruthenium in acid media. J Electroanal Chem Interfacial Electrochem 1984;172(1):211–9. https://doi.org/10.1016/0022-0728(84)80187-4.

[120] Vuković M. Rotating ring–disc electrode study of the enhanced oxygen evolution on an activated ruthenium electrode. J Chem Soc, Faraday Trans 1990;86(22): 3743–6. https://doi.org/10.1039/FT9908603743. 10.1039/FT9908603743.

[121] Liu W, Duan Z, Wang W. Water oxidation-induced surface reconstruction and dissolution at the RuO_2(110) surface revealed by first-principles simulation. J Phys Chem C 2023;127(11):5334–42. https://doi.org/10.1021/acs.jpcc.2c08884.

[122] Hess F, Over H. Coordination inversion of the tetrahedrally coordinated Ru4f surface complex on RuO_2(100) and its decisive role in the anodic corrosion process. ACS Catal 2023;13(5):3433–43. https://doi.org/10.1021/acscatal.2c06260.

[123] Klyukin K, Zagalskaya A, Alexandrov V. Role of dissolution intermediates in promoting oxygen evolution reaction at RuO_2(110) surface. J Phys Chem C 2019; 123(36):22151–7. https://doi.org/10.1021/acs.jpcc.9b03418.

[124] Suntivich J, Hautier G, Dabo I, Crumlin EJ, Kumar D, Cuk T. Probing intermediate configurations of oxygen evolution catalysis across the light spectrum. Nat Energy 2024;9(10):1191–8. https://doi.org/10.1038/s41560-024-01583-x.

[125] Cutsail Iii GE, DeBeer S. Challenges and opportunities for applications of advanced x-ray spectroscopy in catalysis research. ACS Catal 2022;12(10): 5864–86. https://doi.org/10.1021/acscatal.2c01016.

[126] Keßler P, Waldsauer T, Jovic V, Kamp M, Schmitt M, Sing M, Claessen R, Moser S. Epitaxial RuO_2 and IrO_2 films by pulsed laser deposition on TiO_2(110). Apl Mater 2024;12(10). https://doi.org/10.1063/5.0217312. 12/5/2024.

[127] Fields SS, Callahan PG, Combs NG, Cress CD, Bennett SP. Orientation control and mosaicity in heteroepitaxial RuO_2 thin films grown through reactive direct current sputtering. Cryst Growth Des 2024;24(11):4604–12. https://doi.org/10.1021/acs.cgd.4c00271.

[128] Li A, Ooka H, Bonnet N, Hayashi T, Sun Y, Jiang Q, Li C, Han H, Nakamura R. Stable potential windows for long-term electrocatalysis by manganese oxides under acidic conditions. Angew Chem Int Ed 2019;58(15):5054–8. https://doi.org/10.1002/anie.201813361.

[129] Lv H, Wang S, Li J, Shao C, Zhou W, Shen X, Xue M, Zhang C. Self-assembled RuO_2@IrO_x core-shell nanocomposite as high efficient anode catalyst for PEM water electrolyzer. Appl Surf Sci 2020;514:145943. https://doi.org/10.1016/j.apsusc.2020.145943.

[130] Marks LD, Peng L. Nanoparticle shape, thermodynamics and kinetics. J Phys Condens Matter 2016;28(5):053001. https://doi.org/10.1088/0953-8984/28/5/053001.

[131] De Vrieze JE, Gunasooriya GTKK, Thybaut JW, Saeys M. Operando computational catalysis: shape, structure, and coverage under reaction conditions. Curr Opin Chem Eng 2019;23:85–91. https://doi.org/10.1016/j.coche.2019.03.003.

[132] Dedigama I, Angeli P, Ayers K, Robinson JB, Shearing PR, Tsaoulidis D, Brett DJL. In situ diagnostic techniques for characterisation of polymer electrolyte membrane water electrolysers – flow visualisation and electrochemical impedance spectroscopy. Int J Hydrogen Energy 2014;39(9):4468–82. https://doi.org/10.1016/j.ijhydene.2014.01.026.

[133] Nong HN, Oh H-S, Reier T, Willinger E, Willinger M-G, Petkov V, Teschner D, Strasser P. Oxide-supported $IrNiO_x$ core–shell particles as efficient, cost-effective, and stable catalysts for electrochemical water splitting. Angew Chem Int Ed 2015; 54(10):2975–9. https://doi.org/10.1002/anie.201411072. 2022/10/05.

[134] Nong HN, Gan L, Willinger E, Teschner D, Strasser P. IrO_x core-shell nanocatalysts for cost- and energy-efficient electrochemical water splitting. Chem Sci 2014;5 (8):2955–63. https://doi.org/10.1039/C4SC01065E. 10.1039/C4SC01065E.

[135] Reier T, Pawolek Z, Cherevko S, Bruns M, Jones T, Teschner D, Selve S, Bergmann A, Nong HN, Schlögl R, et al. Molecular insight in structure and activity of highly efficient, low-Ir Ir–Ni oxide catalysts for electrochemical water splitting (OER). J Am Chem Soc 2015;137(40):13031–40. https://doi.org/10.1021/jacs.5b07788.

[136] Yu H, Bonville L, Jankovic J, Maric R. Microscopic insights on the degradation of a PEM water electrolyzer with ultra-low catalyst loading. Appl Catal B Environ 2020;260:118194. https://doi.org/10.1016/j.apcatb.2019.118194.

[137] Li N, Araya SS, Kær SK. Long-term contamination effect of iron ions on cell performance degradation of proton exchange membrane water electrolyser. J Power Sources 2019;434:226755. https://doi.org/10.1016/j.jpowsour.2019.226755.

[138] Wu B, Zhao M, Shi W, Liu W, Liu J, Xing D, Yao Y, Hou Z, Ming P, Gu J, et al. The degradation study of Nafion/PTFE composite membrane in PEM fuel cell under accelerated stress tests. Int J Hydrogen Energy 2014;39(26):14381–90. https://doi.org/10.1016/j.ijhydene.2014.02.142.

[139] Weiß A, Siebel A, Bernt M, Shen TH, Tileli V, Gasteiger HA. Impact of intermittent operation on lifetime and performance of a PEM water electrolyzer. J Electrochem Soc 2019;166(8):F487–97. https://doi.org/10.1149/2.0421908jes.

[140] Hongsirikarn K, Goodwin JG, Greenway S, Creager S. Effect of cations (Na^+, Ca^{2+}, Fe^{3+}) on the conductivity of a Nafion membrane. J Power Sources 2010;195(21): 7213–20. https://doi.org/10.1016/j.jpowsour.2010.05.005.

[141] Inazumi C, M H, Kato M, Meazawa S, Sawai N, Oguro K, Takenaka H. The long-term stability of the solid polymer electrolyte water electrolyzer. In: Verzirõglu TN, C. J. W, Baselt JP, Kreysa G, editors. Hydrogen energy progress XI. 1 1996. p. 741.

[142] Rasten E. Electrocatalysis in water electrolysis with solid polymer electrolyte. Norwegian University of Science and Technology; 2001.

[143] Collier A, Wang H, Zi Yuan X, Zhang J, Wilkinson DP. Degradation of polymer electrolyte membranes. Int J Hydrogen Energy 2006;31(13):1838–54. https://doi.org/10.1016/j.ijhydene.2006.05.006.

[144] Saito M, Hayamizu K, Okada T. Temperature dependence of ion and water transport in perfluorinated ionomer membranes for fuel cells. J Phys Chem B 2005;109(8):3112–9. https://doi.org/10.1021/jp045624w.

[145] Suresh G, Pandey AK, Goswami A. Self-diffusion coefficients of water in Nafion-117 membrane with multivalent counterions. J Membr Sci 2006;284(1):193–7. https://doi.org/10.1016/j.memsci.2006.07.031.

[146] Volkov VI, Chernyak AV, Gnezdilov OI, Skirda VD. Hydration, self-diffusion and ionic conductivity of Li^+, Na^+ and Cs^+ cations in Nafion membrane studied by

NMR. Solid State Ionics 2021;364:115627. https://doi.org/10.1016/j.ssi.2021.115627.
[147] Xu S, Wang X, Zhang L, Sun S, Li G, Zhang M, Shao Z-G, Zhu B. The Fe^{3+} role in decreasing the activity of Nafion-bonded IrO_2 catalyst for proton exchange membrane water electrolyser. Int J Hydrogen Energy 2020;45(30):15041–6. https://doi.org/10.1016/j.ijhydene.2020.03.222.
[148] Gubler L, Dockheer SM, Koppenol WH. Radical (HO•, H• and HOO•) formation and ionomer degradation in polymer electrolyte fuel cells. J Electrochem Soc 2011;158(7):B755. https://doi.org/10.1149/1.3581040.
[149] Frensch SH, Serre G, Fouda-Onana F, Jensen HC, Christensen ML, Araya SS, Kær SK. Impact of iron and hydrogen peroxide on membrane degradation for polymer electrolyte membrane water electrolysis: computational and experimental investigation on fluoride emission. J Power Sources 2019;420:54–62. https://doi.org/10.1016/j.jpowsour.2019.02.076.
[150] Li N, Araya SS, Cui X, Kær SK. The effects of cationic impurities on the performance of proton exchange membrane water electrolyzer. J Power Sources 2020;473:228617. https://doi.org/10.1016/j.jpowsour.2020.228617.
[151] Grigoriev SA, Dzhus KA, Bessarabov DG, Millet P. Failure of PEM water electrolysis cells: case study involving anode dissolution and membrane thinning. Int J Hydrogen Energy 2014;39(35):20440–6. https://doi.org/10.1016/j.ijhydene.2014.05.043.
[152] Feng Q, Yuan XZ, Liu G, Wei B, Zhang Z, Li H, Wang H. A review of proton exchange membrane water electrolysis on degradation mechanisms and mitigation strategies. J Power Sources 2017;366:33–55. https://doi.org/10.1016/j.jpowsour.2017.09.006.
[153] Grigoriev SA, Bessarabov DG, Fateev VN. Degradation mechanisms of MEA characteristics during water electrolysis in solid polymer electrolyte cells. Russ J Electrochem 2017;53(3):318–23. https://doi.org/10.1134/S1023193517030065.
[154] Wang X, Zhang L, Li G, Zhang G, Shao Z-G, Yi B. The influence of Ferric ion contamination on the solid polymer electrolyte water electrolysis performance. Electrochim Acta 2015;158:253–7. https://doi.org/10.1016/j.electacta.2015.01.140.
[155] Kexin Z, Xiao L, Lina W, Ke S, Yuannan W, Zhoubing X, Qiannan W, Xinyu B, Mohamed S H, Hui C. Status and perspectives of key materials for PEM electrolyzer. Nano Res Energy 2022. https://doi.org/10.26599/NRE.2022.9120032.
[156] Wei G, Wang Y, Huang C, Gao Q, Wang Z, Xu L. The stability of MEA in SPE water electrolysis for hydrogen production. Int J Hydrogen Energy 2010;35(9):3951–7. https://doi.org/10.1016/j.ijhydene.2010.01.153.
[157] Rakousky C, Keeley GP, Wippermann K, Carmo M, Stolten D. The stability challenge on the pathway to high-current-density polymer electrolyte membrane water electrolyzers. Electrochim Acta 2018;278:324–31. https://doi.org/10.1016/j.electacta.2018.04.154.
[158] Song J, Wei C, Huang Z-F, Liu C, Zeng L, Wang X, Xu ZJ. A review on fundamentals for designing oxygen evolution electrocatalysts. Chem Soc Rev 2020;49(7):2196–214. https://doi.org/10.1039/C9CS00607A. 10.1039/C9CS00607A.
[159] Baik C, Lee SW, Pak C. Control of the pore size distribution inside the RuO_2 catalyst by using silica nanosphere particle for highly efficient water electrolysis. Microporous Mesoporous Mater 2020;309:110567. https://doi.org/10.1016/j.micromeso.2020.110567.
[160] Ge R, Li L, Su J, Lin Y, Tian Z, Chen L. Ultrafine defective RuO_2 electrocatayst integrated on carbon cloth for robust water oxidation in acidic media. Adv Energy Mater 2019;9(35):1901313. https://doi.org/10.1002/aenm.201901313.
[161] Zhao ZL, Wang Q, Huang X, Feng Q, Gu S, Zhang Z, Xu H, Zeng L, Gu M, Li H. Boosting the oxygen evolution reaction using defect-rich ultra-thin ruthenium oxide nanosheets in acidic media. Energy Environ Sci 2020;13(12):5143–51. https://doi.org/10.1039/D0EE01960G. 10.1039/D0EE01960G.
[162] Lodi G, Sivieri E, De Battisti A, Trasatti S. Ruthenium dioxide-based film electrodes. J Appl Electrochem 1978;8(2):135–43. https://doi.org/10.1007/BF00617671.
[163] Lee Y, Suntivich J, May KJ, Perry EE, Shao-Horn Y. Synthesis and activities of rutile IrO_2 and RuO_2 nanoparticles for oxygen evolution in acid and alkaline solutions. J Phys Chem Lett 2012;3(3):399–404. https://doi.org/10.1021/jz2016507.
[164] Geiger S, Kasian O, Ledendecker M, Pizzutilo E, Mingers AM, Fu WT, Diaz-Morales O, Li Z, Oellers T, Fruchter L, Mayrhofer KJJ, Koper MTM, Cherevko S. The stability number as a metric for electrocatalyst stability benchmarking. Nat Catal 2018;1(7):508–15. https://doi.org/10.1038/s41929-018-0085-6.
[165] Tsuji E, Imanishi A, Fukui K-i, Nakato Y. Electrocatalytic activity of amorphous RuO_2 electrode for oxygen evolution in an aqueous solution. Electrochim Acta 2011;56(5):2009–16. https://doi.org/10.1016/j.electacta.2010.11.062.
[166] Tamura H, Iwakura C. Metal oxide anodes for oxygen evolution. Int J Hydrogen Energy 1982;7(11):857–65. https://doi.org/10.1016/0360-3199(82)90003-9.
[167] Koper MTM. Thermodynamic theory of multi-electron transfer reactions: implications for electrocatalysis. J Electroanal Chem 2011;660(2):254–60. https://doi.org/10.1016/j.jelechem.2010.10.004.
[168] Alia SM, Anderson GC. Iridium oxygen evolution activity and durability baselines in rotating disk electrode half-cells. J Electrochem Soc 2019;166(4):F282. https://doi.org/10.1149/2.0731904jes.
[169] Adams R, Shriner RL. Platinum oxide as a catalyst in the reduction of organic compounds. III. Preparation and properties of the oxide of platinum obtained by the fusion of chloroplatinic acid with sodium nitrate. J Am Chem Soc 1923;45(9):2171–9. https://doi.org/10.1021/ja01662a022.
[170] Soudens FA, Karels S, Felix C, Pasupathi S. Development of unsupported Ru and Ni based oxides with enhanced performance for the oxygen evolution reaction in acidic media. Electrocatalysis 2023;14(3):437–47. https://doi.org/10.1007/s12678-022-00798-4.
[171] Pham TS, Pham HH, Do CL, Anh TNT, Pham TA. $Ir_xRu_{1-x}O_2$ nanoparticles with enhanced electrocatalytic properties for the oxygen evolution reaction in proton exchange membrane water electrolysis. J Electron Mater 2021;50(3):1239–46. https://doi.org/10.1007/s11664-020-08624-7.
[172] Angelinetta C, Trasatti S, Atanasoska LD, Minevski ZS, Atanasoski RT. Effect of preparation on the surface and electrocatalytic properties of $RuO_2 + IrO_2$ mixed oxide electrodes. Mater Chem Phys 1989;22(1):231–47. https://doi.org/10.1016/0254-0584(89)90039-4.
[173] Tesch MF, Neugebauer S, Narangoda PV, Schlögl R, Mechler AK. The rotating disc electrode: measurement protocols and reproducibility in the evaluation of catalysts for the oxygen evolution reaction. Energy Adv 2023;2(11):1823–30. https://doi.org/10.1039/D3YA00340J. 10.1039/D3YA00340J.
[174] Etzi Coller Pascuzzi M, Goryachev A, Hofmann JP, Hensen EJM. Mn promotion of rutile TiO_2-RuO_2 anodes for water oxidation in acidic media. Appl Catal B Environ 2020;261:118225. https://doi.org/10.1016/j.apcatb.2019.118225.
[175] Lebedev D, Povia M, Waltar K, Abdala PM, Castelli IE, Fabbri E, Blanco MV, Fedorov A, Copéret C, Marzari N, et al. Highly active and stable iridium pyrochlores for oxygen evolution reaction. Chem Mater 2017;29(12):5182–91. https://doi.org/10.1021/acs.chemmater.7b00766.
[176] Abbott DF, Pittkowski RK, Macounová K, Nebel R, Marelli E, Fabbri E, Castelli IE, Krtil P, Schmidt TJ. Design and synthesis of Ir/Ru pyrochlore catalysts for the oxygen evolution reaction based on their bulk thermodynamic properties. ACS Appl Mater Interfaces 2019;11(41):37748–60. https://doi.org/10.1021/acsami.9b13220.
[177] Zhang N, Wang C, Chen J, Hu C, Ma J, Deng X, Qiu B, Cai L, Xiong Y, Chai Y. Metal substitution steering electron correlations in pyrochlore ruthenates for efficient acidic water oxidation. ACS Nano 2021;15(5):8537–48. https://doi.org/10.1021/acsnano.1c00266.
[178] Jin R, Zeng C, Zhou M, Chen Y. Atomically precise colloidal metal nanoclusters and nanoparticles: fundamentals and opportunities. Chem Rev 2016;116(18):10346–413. https://doi.org/10.1021/acs.chemrev.5b00703.
[179] Chakraborty I, Pradeep T. Atomically precise clusters of noble metals: emerging link between atoms and nanoparticles. Chem Rev 2017;117(12):8208–71. https://doi.org/10.1021/acs.chemrev.6b00769.
[180] Luu TL, Kim C, Kim J, Kim S, Yoon J. The Effect of preparation parameters in thermal decomposition of ruthenium dioxide electrodes on chlorine electrocatalytic activity. Bull Kor Chem Soc 2015;36(5):1411–7. https://doi.org/10.1002/bkcs.10275.
[181] Gupta SK, Mao Y. A review on molten salt synthesis of metal oxide nanomaterials: status, opportunity, and challenge. Prog Mater Sci 2021;117:100734. https://doi.org/10.1016/j.pmatsci.2020.100734.
[182] Puthiyapura VK, Pasupathi S, Su H, Liu X, Pollet B, Scott K. Investigation of supported IrO_2 as electrocatalyst for the oxygen evolution reaction in proton exchange membrane water electrolyser. Int J Hydrogen Energy 2014;39(5):1905–13. https://doi.org/10.1016/j.ijhydene.2013.11.056.
[183] Liz-Marzán LM, Kagan CR, Millstone JE. Reproducibility in nanocrystal synthesis? Watch out for impurities. ACS Nano 2020;14(6):6359–61. https://doi.org/10.1021/acsnano.0c04709.
[184] Su J, Ge R, Jiang K, Dong Y, Hao F, Tian Z, Chen G, Chen L. Assembling ultrasmall copper-doped ruthenium oxide nanocrystals into hollow porous polyhedra: highly robust electrocatalysts for oxygen evolution in acidic media. Adv Mater 2018;30(29):1801351. https://doi.org/10.1002/adma.201801351.
[185] Song XZ, Zhang N, Wang XF, Tan Z. Recent advances of metal-organic frameworks and their composites toward oxygen evolution electrocatalysis. Mater Today Energy 2021;19:100597. https://doi.org/10.1016/j.mtener.2020.100597.
[186] Luo J, Waterhouse GIN, Peng L, Chen Q. Recent progress in high-loading single-atom catalysts and their applications. Indus Chem Mater 2023;1(4):486–500. https://doi.org/10.1039/D3IM00062A. 10.1039/D3IM00062A.
[187] Speck FD, Kim JH, Bae G, Joo SH, Mayrhofer KJJ, Choi CH, Cherevko S. Single-atom catalysts: a perspective toward application in electrochemical energy conversion. JACS Au 2021;1(8):1086–100. https://doi.org/10.1021/jacsau.1c00121.
[188] Li J, Chen C, Xu L, Zhang Y, Wei W, Zhao E, Wu Y, Chen C. Challenges and perspectives of single-atom-based catalysts for electrochemical reactions. JACS Au 2023;3(3):736–55. https://doi.org/10.1021/jacsau.3c00001.
[189] Bernt M, Gasteiger HA. Influence of ionomer content in IrO_2/TiO_2 electrodes on PEM water electrolyzer performance. J Electrochem Soc 2016;163(11):F3179. https://doi.org/10.1149/2.0231611jes.
[190] Jiménez-Morales I, Cavaliere S, Dupont M, Jones D, Rozière J. On the stability of antimony doped tin oxide supports in proton exchange membrane fuel cell and water electrolysers. Sustain Energy Fuels 2019;3(6):1526–35. https://doi.org/10.1039/C8SE00619A. 10.1039/C8SE00619A.
[191] Thomassen MS, Mokkelbost T, Sheridan E, Lind A. Supported nanostructured Ir and IrRu electrocatalysts for oxygen evolution in PEM electrolysers. ECS Trans 2011;35(34):271–9. https://doi.org/10.1149/1.3654225.
[192] Xu J, Liu G, Li J, Wang X. The electrocatalytic properties of an IrO_2/SnO_2 catalyst using SnO_2 as a support and an assisting reagent for the oxygen evolution reaction. Electrochim Acta 2012;59:105–12. https://doi.org/10.1016/j.electacta.2011.10.044.
[193] Moriau L, Smiljanić M, Lončar A, Hodnik N. Supported iridium-based oxygen evolution reaction electrocatalysts - recent developments. ChemCatChem 2022;14:e202200586. https://doi.org/10.1002/cctc.202200586.
[194] Sun W, Zhou Z, Zaman WQ, Cao L-m, Yang J. Rational Manipulation of IrO_2 lattice strain on α-MnO_2 nanorods as a highly efficient water-splitting catalyst.

ACS Appl Mater Interfaces 2017;9(48):41855–62. https://doi.org/10.1021/acsami.7b12775.
[195] Vinod M, Gopchandran KG. Ag@Au core–shell nanoparticles synthesized by pulsed laser ablation in water: effect of plasmon coupling and their SERS performance. Spectrochim Acta Mol Biomol Spectrosc 2015;149:913–9. https://doi.org/10.1016/j.saa.2015.05.004.
[196] Huang B, Xu H, Jiang N, Wang M, Huang J, Guan L. Tensile-strained RuO_2 loaded on antimony-tin oxide by fast quenching for proton-exchange membrane Water Electrolyzer. Adv Sci 2022;9(23):2201654. https://doi.org/10.1002/advs.202201654.
[197] Hu W, Chen S, Xia Q. IrO_2/Nb–TiO_2 electrocatalyst for oxygen evolution reaction in acidic medium. Int J Hydrogen Energy 2014;39(13):6967–76. https://doi.org/10.1016/j.ijhydene.2014.02.114.
[198] Polonský J, Petrushina IM, Christensen E, Bouzek K, Prag CB, Andersen JET, Bjerrum NJ. Tantalum carbide as a novel support material for anode electrocatalysts in polymer electrolyte membrane water electrolysers. Int J Hydrogen Energy 2012;37(3):2173–81. https://doi.org/10.1016/j.ijhydene.2011.11.035.
[199] Long X, Zhao B, Zhao Q, Wu X, Zhu M-N, Feng R, Shakouri M, Zhang Y, Xiao X, Zhang J, et al. Ru-RuO_2 nano-heterostructures stabilized by the sacrificing oxidation strategy of Mn_3O_4 substrate for boosting acidic oxygen evolution reaction. Appl Catal B Environ 2024;343:123559. https://doi.org/10.1016/j.apcatb.2023.123559.
[200] Pham CV, Bühler M, Knöppel J, Bierling M, Seeberger D, Escalera-López D, Mayrhofer KJJ, Cherevko S, Thiele S. IrO_2 coated TiO_2 core-shell microparticles advance performance of low loading proton exchange membrane water electrolyzers. Appl Catal B Environ 2020;269:118762. https://doi.org/10.1016/j.apcatb.2020.118762.
[201] Geiger S, Kasian O, Mingers AM, Mayrhofer KJJ, Cherevko S. Stability limits of tin-based electrocatalyst supports. Sci Rep 2017;7(1):4595. https://doi.org/10.1038/s41598-017-04079-9.
[202] Oh H-S, Nong HN, Reier T, Bergmann A, Gliech M, Ferreira de Araújo J, Willinger E, Schlögl R, Teschner D, Strasser P. Electrochemical catalyst–support effects and their stabilizing role for IrO_x nanoparticle catalysts during the oxygen evolution reaction. J Am Chem Soc 2016;138(38):12552–63. https://doi.org/10.1021/jacs.6b07199.
[203] Siracusano S, Baglio V, D'Urso C, Antonucci V, Aricò AS. Preparation and characterization of titanium suboxides as conductive supports of IrO_2 electrocatalysts for application in SPE electrolysers. Electrochim Acta 2009;54(26):6292–9. https://doi.org/10.1016/j.electacta.2009.05.094.
[204] Daiane Ferreira da Silva C, Claudel F, Martin V, Chattot R, Abbou S, Kumar K, Jiménez-Morales I, Cavaliere S, Jones D, Rozière J, et al. Oxygen evolution reaction activity and stability benchmarks for supported and unsupported IrOx electrocatalysts. ACS Catal 2021;11(7):4107–16. https://doi.org/10.1021/acscatal.0c04613.
[205] Riva M, Kubicek M, Hao X, Franceschi G, Gerhold S, Schmid M, Hutter H, Fleig J, Franchini C, Yildiz B, et al. Influence of surface atomic structure demonstrated on oxygen incorporation mechanism at a model perovskite oxide. Nat Commun 2018;9(1):3710. https://doi.org/10.1038/s41467-018-05685-5.
[206] Riva M, Franceschi G, Lu Q, Schmid M, Yildiz B, Diebold U. Pushing the detection of cation nonstoichiometry to the limit. Phys Rev Mater 2019;3(4):043802. https://doi.org/10.1103/PhysRevMaterials.3.043802.
[207] Sokolović I, Franceschi G, Wang Z, Xu J, Pavelec J, Riva M, Schmid M, Diebold U, Setvín M. Quest for a pristine unreconstructed $SrTiO_3$(001) surface: an atomically resolved study via noncontact atomic force microscopy. Phys Rev B 2021;103(24):L241406. https://doi.org/10.1103/PhysRevB.103.L241406.
[208] Ruban AV, Skriver HL, Nørskov JK. Surface segregation energies in transition-metal alloys. Phys Rev B 1999;59(24):15990–6000. https://doi.org/10.1103/PhysRevB.59.15990.
[209] Danilovic N, Subbaraman R, Chang KC, Chang SH, Kang Y, Snyder J, Paulikas AP, Strmcnik D, Kim YT, Myers D, et al. Using surface segregation to design stable ru-ir oxides for the oxygen evolution reaction in acidic environments. Angew Chem Int Ed 2014;53(51):14016–21. https://doi.org/10.1002/anie.201406455.
[210] Owe L-E, Tsypkin M, Wallwork KS, Haverkamp RG, Sunde S. Iridium–ruthenium single phase mixed oxides for oxygen evolution: composition dependence of electrocatalytic activity. Electrochim Acta 2012;70:158–64. https://doi.org/10.1016/j.electacta.2012.03.041.
[211] Gaudet J, Tavares AC, Trasatti S, Guay D. Physicochemical characterization of mixed RuO_2 SnO_2 solid solutions. Chem Mater 2005;17(6):1570–9. https://doi.org/10.1021/cm048129l.
[212] Ardizzone S, Bianchi CL, Borgese L, Cappelletti G, Locatelli C, Minguzzi A, Rondinini S, Vertova A, Ricci PC, Cannas C, et al. Physico-chemical characterization of IrO_2–SnO_2 sol-gel nanopowders for electrochemical applications. J Appl Electrochem 2009;39(11):2093–105. https://doi.org/10.1007/s10800-009-9895-1.
[213] Nguyen TD, Nguyen HH, Dai C, Wang J, Scherer GG. Activity and stability optimization of $Ru_xIr_{1-x}O_2$ nanocatalyst for the oxygen evolution reaction by tuning the synthetic process. Int J Hydrogen Energy 2020;45(1):46–55. https://doi.org/10.1016/j.ijhydene.2019.10.179.
[214] Xu L, Xin Y, Wang J. A comparative study on IrO_2–Ta_2O_5 coated titanium electrodes prepared with different methods. Electrochim Acta 2009;54(6):1820–5. https://doi.org/10.1016/j.electacta.2008.10.004.
[215] Fadley CS. X-ray photoelectron spectroscopy: progress and perspectives. J Electron Spectrosc Relat Phenom 2010;178–179:2–32. https://doi.org/10.1016/j.elspec.2010.01.006.
[216] Chang C-J, Chu Y-C, Yan H-Y, Liao Y-F, Chen HM. Revealing the structural transformation of rutile RuO_2 via in situ X-ray absorption spectroscopy during the oxygen evolution reaction. Dalton Trans 2019;48(21):7122–9. https://doi.org/10.1039/C9DT00138G. 10.1039/C9DT00138G.
[217] Katsounaros I, Cherevko S, Zeradjanin AR, Mayrhofer KJJ. Oxygen electrochemistry as a cornerstone for sustainable energy conversion. Angew Chem Int Ed 2014;53(1):102–21. https://doi.org/10.1002/anie.201306588.
[218] An L, Yang F, Fu C, Cai X, Shen S, Xia G, Li J, Du Y, Luo L, Zhang J. A functionally stable RuMn electrocatalyst for oxygen evolution reaction in acid. Adv Funct Mater 2022;32(27):2200131. https://doi.org/10.1002/adfm.202200131.
[219] Tao F, Grass ME, Zhang Y, Butcher DR, Renzas JR, Liu Z, Chung JY, Mun BS, Salmeron M, Somorjai GA. Reaction-driven restructuring of Rh-Pd and Pt-Pd core-shell nanoparticles. Science 2008;322(5903):932–4. https://doi.org/10.1126/science.1164170.
[220] May KJ, Carlton CE, Stoerzinger KA, Risch M, Suntivich J, Lee Y-L, Grimaud A, Shao-Horn Y. Influence of oxygen evolution during water oxidation on the surface of perovskite oxide catalysts. J Phys Chem Lett 2012;3(22):3264–70. https://doi.org/10.1021/jz301414z.
[221] Wang Y, Gong T, Lee M, Hall AS. Structural transformations of metal alloys under electrocatalytic conditions. Curr Opin Electrochem 2021;30:100796. https://doi.org/10.1016/j.coelec.2021.100796.
[222] Hodnik N, Jovanovič P, Pavlišič A, Jozinović B, Zorko M, Bele M, Šelih VS, Šala M, Hočevar S, Gaberšček M. New insights into corrosion of ruthenium and ruthenium oxide nanoparticles in acidic media. J Phys Chem C 2015;119(18):10140–7. https://doi.org/10.1021/acs.jpcc.5b01832.
[223] Kötz R, Lewerenz HJ, Brüesch P, Stucki S. Oxygen evolution on Ru and Ir electrodes: XPS-studies. J Electroanal Chem Interfacial Electrochem 1983;150(1):209–16. https://doi.org/10.1016/S0022-0728(83)80203-4.
[224] Saveleva VA, Wang L, Luo W, Zafeiratos S, Ulhaq-Bouillet C, Gago AS, Friedrich KA, Savinova ER. Uncovering the stabilization mechanism in bimetallic ruthenium–iridium anodes for proton exchange membrane electrolyzers. J Phys Chem Lett 2016;7(16):3240–5. https://doi.org/10.1021/acs.jpclett.6b01500.
[225] Lin Z, Liu S, Liu Y, Liu Z, Zhang S, Zhang X, Tian Y, Tang Z. Rational design of Ru aerogel and RuCo aerogels with abundant oxygen vacancies for hydrogen evolution reaction, oxygen evolution reaction, and overall water splitting. J Power Sources 2021;514:230600. https://doi.org/10.1016/j.jpowsour.2021.230600.
[226] Yan S, Liao W, Zhong M, Li W, Wang C, Pinna N, Chen W, Lu X. Partially oxidized ruthenium aerogel as highly active bifunctional electrocatalyst for overall water splitting in both alkaline and acidic media. Appl Catal B Environ 2022;307:121199. https://doi.org/10.1016/j.apcatb.2022.121199.
[227] Jiang R, Tran DT, Li J, Chu D. Ru@RuO_2 Core-Shell Nanorods: a highly active and stable bifunctional catalyst for oxygen evolution and hydrogen evolution reactions. Energy Environ Mater 2019;2(3):201–8. https://doi.org/10.1002/eem2.12031.
[228] Fan Z, Jiang J, Ai L, Shao Z, Liu S. Rational design of ruthenium and cobalt-based composites with rich metal–insulator interfaces for efficient and stable overall water splitting in acidic electrolyte. ACS Appl Mater Interfaces 2019;11(51):47894–903. https://doi.org/10.1021/acsami.9b15844.
[229] Chen M, Fan Z, Ai L, Jiang J. Spatial confinement of partially oxidized RuCo alloys in N-doped carbon frameworks for highly efficient oxygen evolution electrocatalysis under acidic conditions. Appl Surf Sci 2021;564:150478. https://doi.org/10.1016/j.apsusc.2021.150478.
[230] Hao S, Liu M, Pan J, Liu X, Tan X, Xu N, He Y, Lei L, Zhang X. Dopants fixation of ruthenium for boosting acidic oxygen evolution stability and activity. Nat Commun 2020;11(1):5368. https://doi.org/10.1038/s41467-020-19212-y.
[231] Sun Y, Zhang Y, Liu C-X, Felser C, Yan B. Dirac nodal lines and induced spin Hall effect in metallic rutile oxides. Phys Rev B 2017;95(23):235104. https://doi.org/10.1103/PhysRevB.95.235104.
[232] Karube S, Tanaka T, Sugawara D, Kadoguchi N, Kohda M, Nitta J. Observation of spin-splitter torque in collinear antiferromagnetic RuO_2. Phys Rev Lett 2022;129(13):137201. https://doi.org/10.1103/PhysRevLett.129.137201.
[233] Keßler P, Garcia-Gassull L, Suter A, Prokscha T, Salman Z, Khalyavin D, Manuel P, Orlandi F, Mazin II, Valentí R, et al. Absence of magnetic order in RuO_2: insights from μSR spectroscopy and neutron diffraction. npj Spintronics 2024;2(1):50. https://doi.org/10.1038/s44306-024-00055-y.
[234] Tschirner T, Keßler P, Gonzalez Betancourt RD, Kotte T, Kriegner D, Büchner B, Dufouleur J, Kamp M, Jovic V, Smejkal L, et al. Saturation of the anomalous Hall effect at high magnetic fields in altermagnetic RuO_2. Apl Mater 2023;11(10). https://doi.org/10.1063/5.0160335. 12/9/2024.
[235] Petrykin V, Macounová K, Okube M, Mukerjee S, Krtil P. Local structure of Co doped RuO_2 nanocrystalline electrocatalytic materials for chlorine and oxygen evolution. Catal Today 2013;202:63–9. https://doi.org/10.1016/j.cattod.2012.03.075.
[236] Zeradjanin AR, Masa J, Spanos I, Schlögl R. Activity and stability of oxides during oxygen evolution reaction---from mechanistic controversies toward relevant electrocatalytic descriptors. Front Energy Res 2021;8:Review. https://doi.org/10.3389/fenrg.2020.613092.
[237] Cheng J, Zhang H, Chen G, Zhang Y. Study of $Ir_xRu_{1-x}O_2$ oxides as anodic electrocatalysts for solid polymer electrolyte water electrolysis. Electrochim Acta 2009;54(26):6250–6. https://doi.org/10.1016/j.electacta.2009.05.090.
[238] Godínez-Salomón JF, Ospina-Acevedo F, Albiter LA, Bailey KO, Naymik ZG, Mendoza-Cruz R, Balbuena PB, Rhodes CP. Titanium substitution effects on the structure, activity, and stability of nanoscale ruthenium oxide oxygen evolution electrocatalysts: experimental and computational study. ACS Appl Nano Mater 2022;5(8):11752–75. https://doi.org/10.1021/acsanm.2c02760.

[239] Trasatti S. Electrocatalysis: understanding the success of DSA. Electrochim Acta 2000;45(15):2377–85. https://doi.org/10.1016/S0013-4686(00)00338-8.

[240] Escalera-López D, Czioska S, Geppert J, Boubnov A, Röse P, Saraçi E, Krewer U, Grunwaldt J-D, Cherevko S. Phase- and surface composition-dependent electrochemical stability of Ir-Ru nanoparticles during oxygen evolution reaction. ACS Catal 2021;11(15):9300–16. https://doi.org/10.1021/acscatal.1c01682.

[241] Kasian O, Geiger S, Stock P, Polymeros G, Breitbach B, Savan A, Ludwig A, Cherevko S, Mayrhofer KJJ. On the origin of the improved ruthenium stability in RuO_2–IrO_2 mixed oxides. J Electrochem Soc 2016;163(11):F3099–104. https://doi.org/10.1149/2.0131611jes.

[242] Escudero-Escribano M, Pedersen AF, Paoli EA, Frydendal R, Friebel D, Malacrida P, Rossmeisl J, Stephens IEL, Chorkendorff I. Importance of surface IrO_x in stabilizing RuO_2 for oxygen evolution. J Phys Chem B 2018;122(2):947–55. https://doi.org/10.1021/acs.jpcb.7b07047.

[243] Gloag L, Benedetti TM, Cheong S, Li Y, Chan X-H, Lacroix L-M, Chang SLY, Arenal R, Florea I, Barron H, et al. Three-dimensional branched and faceted gold–ruthenium nanoparticles: using nanostructure to improve stability in oxygen evolution electrocatalysis. Angew Chem Int Ed 2018;57(32):10241–5. https://doi.org/10.1002/anie.201806300.

[244] Wu Q, Jiang K, Han J, Chen D, Luo M, Lan J, Peng M, Tan Y. Dynamic shrinkage of metal-oxygen bonds in atomic Co-doped nanoporous RuO_2 for acidic oxygen evolution. Sci China Mater 2022;65(5):1262–8. https://doi.org/10.1007/s40843-021-1912-8.

[245] Ko Y-J, Han MH, Lim C, Yu S-H, Choi CH, Min BK, Choi J-Y, Lee WH, Oh H-S. Unveiling the role of Ni in Ru-Ni oxide for oxygen evolution: lattice oxygen participation enhanced by structural distortion. J Energy Chem 2023;77:54–61. https://doi.org/10.1016/j.jechem.2022.09.032.

[246] Joo J, Park Y, Kim J, Kwon T, Jun M, Ahn D, Baik H, Jang JH, Kim JY, Lee K. Mn-dopant differentiating the Ru and Ir oxidation states in catalytic oxides toward durable oxygen evolution reaction in acidic electrolyte. Small Methods 2022;6(1):2101236. https://doi.org/10.1002/smtd.202101236.

[247] Wen Y, Chen P, Wang L, Li S, Wang Z, Abed J, Mao X, Min Y, Dinh CT, Luna PD, et al. Stabilizing highly active ru sites by suppressing lattice oxygen participation in acidic water oxidation. J Am Chem Soc 2021;143(17):6482–90. https://doi.org/10.1021/jacs.1c00384.

[248] Kim B-J, Abbott DF, Cheng X, Fabbri E, Nachtegaal M, Bozza F, Castelli IE, Lebedev D, Schäublin R, Copéret C, et al. Unraveling thermodynamics, stability, and oxygen evolution activity of strontium ruthenium perovskite oxide. ACS Catal 2017;7(5):3245–56. https://doi.org/10.1021/acscatal.6b03171.

[249] Ji M, Yang X, Chang S, Chen W, Wang J, He D, Hu Y, Deng Q, Sun Y, Li B, et al. RuO_2 clusters derived from bulk $SrRuO_3$: robust catalyst for oxygen evolution reaction in acid. Nano Res 2022;15(3):1959–65. https://doi.org/10.1007/s12274-021-3843-8.

[250] Shang C, Cao C, Yu D, Yan Y, Lin Y, Li H, Zheng T, Yan X, Yu W, Zhou S, et al. Electron correlations engineer catalytic activity of pyrochlore iridates for acidic water oxidation. Adv Mater 2019;31(6):1805104. https://doi.org/10.1002/adma.201805104.

[251] Li P, Wang M, Duan X, Zheng L, Cheng X, Zhang Y, Kuang Y, Li Y, Ma Q, Feng Z, et al. Boosting oxygen evolution of single-atomic ruthenium through electronic coupling with cobalt-iron layered double hydroxides. Nat Commun 2019;10(1):1711. https://doi.org/10.1038/s41467-019-09666-0.

[252] Yao Y, Hu S, Chen W, Huang Z-Q, Wei W, Yao T, Liu R, Zang K, Wang X, Wu G, et al. Engineering the electronic structure of single atom Ru sites via compressive strain boosts acidic water oxidation electrocatalysis. Nat Catal 2019;2(4):304–13. https://doi.org/10.1038/s41929-019-0246-2.

[253] Yang Y, Yang Q-N, Yang Y-B, Guo P-F, Feng W-X, Jia Y, Wang K, Wang W-T, He Z-H, Liu Z-T. Enhancing water oxidation of Ru single atoms via oxygen-coordination bonding with NiFe layered double hydroxide. ACS Catal 2023;13(4):2771–9. https://doi.org/10.1021/acscatal.2c05624.

[254] Hao Y, Hung S-F, Zeng W-J, Wang Y, Zhang C, Kuo C-H, Wang L, Zhao S, Zhang Y, Chen H-Y, et al. Switching the oxygen evolution mechanism on atomically dispersed Ru for enhanced acidic reaction kinetics. J Am Chem Soc 2023;145(43):23659–69. https://doi.org/10.1021/jacs.3c07777.

[255] Rong C, Shen X, Wang Y, Thomsen L, Zhao T, Li Y, Lu X, Amal R, Zhao C. Electronic structure engineering of single-atom Ru sites via Co–N4 sites for bifunctional pH-universal water splitting. Adv Mater 2022;34(21):2110103. https://doi.org/10.1002/adma.202110103.

[256] Cao L, Luo Q, Chen J, Wang L, Lin Y, Wang H, Liu X, Shen X, Zhang W, Liu W, et al. Dynamic oxygen adsorption on single-atomic Ruthenium catalyst with high performance for acidic oxygen evolution reaction. Nat Commun 2019;10(1):4849. https://doi.org/10.1038/s41467-019-12886-z.

[257] Zhai P, Xia M, Wu Y, Zhang G, Gao J, Zhang B, Cao S, Zhang Y, Li Z, Fan Z, et al. Engineering single-atomic ruthenium catalytic sites on defective nickel-iron layered double hydroxide for overall water splitting. Nat Commun 2021;12(1):4587. https://doi.org/10.1038/s41467-021-24828-9.

[258] An L, Cai X, Shen S, Yin J, Jiang K, Zhang J. Dealloyed $RuNiO_x$ as a robust electrocatalyst for the oxygen evolution reaction in acidic media. Dalton Trans 2021;50(15):5124–7. https://doi.org/10.1039/D1DT00195G. 10.1039/D1DT00195G.

[259] Tomboc GM, Kim T, Jung S, Yoon HJ, Lee K. Modulating the local coordination environment of single-atom catalysts for enhanced catalytic performance in hydrogen/oxygen evolution reaction. Small 2022;18(17):2105680. https://doi.org/10.1002/smll.202105680.

[260] Wei X, Luo X, Wu N, Gu W, Lin Y, Zhu C. Recent advances in synergistically enhanced single-atomic site catalysts for boosted oxygen reduction reaction. Nano Energy 2021;84:105817. https://doi.org/10.1016/j.nanoen.2021.105817.

[261] Baturina O, Lu Q, Xu F, Purdy A, Dyatkin B, Sang X, Unocic R, Brintlinger T, Gogotsi Y. Effect of nanostructured carbon support on copper electrocatalytic activity toward CO_2 electroreduction to hydrocarbon fuels. Catal Today 2017;288:2–10. https://doi.org/10.1016/j.cattod.2016.11.001.

[262] Yang Y, Luo M, Zhang W, Sun Y, Chen X, Guo S. Metal surface and interface energy electrocatalysis: fundamentals, performance engineering, and opportunities. Chem 2018;4(9):2054–83. https://doi.org/10.1016/j.chempr.2018.05.019.

[263] Koper MTM. Structure sensitivity and nanoscale effects in electrocatalysis. Nanoscale 2011;3(5):2054–73. https://doi.org/10.1039/C0NR00857E. 10.1039/C0NR00857E.

[264] Reiser C, Keßler P, Kamp M, Jovic V, Moser S. Specific capacitance of RuO_2(110) depends sensitively on surface order. J Phys Chem C 2023;127(7):3682–8. https://doi.org/10.1021/acs.jpcc.2c07217.

[265] Roduner E. Understanding catalysis. Chem Soc Rev 2014;43(24):8226–39. https://doi.org/10.1039/C4CS00210E. 10.1039/C4CS00210E.

[266] Portela R, Perez-Ferreras S, Serrano-Lotina A, Bañares MA. Engineering operando methodology: understanding catalysis in time and space. Front Chem Sci Eng 2018;12(3):509–36. https://doi.org/10.1007/s11705-018-1740-9.

[267] Felix C, Bladergroen BJ, Linkov V, Pollet BG, Pasupathi S. Ex-situ electrochemical characterization of IrO_2 synthesized by a modified adams fusion method for the oxygen evolution reaction. Catalysts 2019;9(4):318.

[268] Ruiz Esquius J, Morgan DJ, Spanos I, Hewes DG, Freakley SJ, Hutchings GJ. Effect of base on the facile hydrothermal preparation of highly active IrO_x oxygen evolution catalysts. ACS Appl Energy Mater 2020;3(1):800–9. https://doi.org/10.1021/acsaem.9b01642.

[269] Peterson AA, Vogel F, Lachance RP, Fröling M, Antal JMJ, Tester JW. Thermochemical biofuel production in hydrothermal media: a review of sub- and supercritical water technologies. Energy Environ Sci 2008;1(1):32–65. https://doi.org/10.1039/B810100K. 10.1039/B810100K.

[270] Védrine JC. Revisiting active sites in heterogeneous catalysis: their structure and their dynamic behaviour. Appl Catal Gen 2014;474:40–50. https://doi.org/10.1016/j.apcata.2013.05.029.

[271] Vogt C, Weckhuysen BM. The concept of active site in heterogeneous catalysis. Nat Rev Chem 2022;6(2):89–111. https://doi.org/10.1038/s41570-021-00340-y.

[272] Wei C, Rao RR, Peng J, Huang B, Stephens IEL, Risch M, Xu ZJ, Shao-Horn Y. Recommended practices and benchmark activity for hydrogen and oxygen electrocatalysis in water splitting and fuel cells. Adv Mater 2019;31(31):1806296. https://doi.org/10.1002/adma.201806296.

[273] Luber EJ, Buriak JM. Reporting performance in organic photovoltaic devices. ACS Nano 2013;7(6):4708–14. https://doi.org/10.1021/nn402883g.

[274] Qureshi M, Takanabe K. Insights on measuring and reporting heterogeneous photocatalysis: efficiency definitions and setup examples. Chem Mater 2017;29(1):158–67. https://doi.org/10.1021/acs.chemmater.6b02907.

[275] Buriak JM, Jones CW, Kamat PV, Schanze KS, Schatz GC, Scholes GD, Weiss PS. Virtual issue on best practices for reporting the properties of materials and devices. Chem Mater 2016;28(11):3525–6. https://doi.org/10.1021/acs.chemmater.6b01854.

[276] Christians JA, Manser JS, Kamat PV. Best Practices in perovskite solar cell efficiency measurements. Avoiding the error of making bad cells look good. J Phys Chem Lett 2015;6(5):852–7. https://doi.org/10.1021/acs.jpclett.5b00289.

[277] Arminio-Ravelo JA, Jensen AW, Jensen KD, Quinson J, Escudero-Escribano M. Electrolyte effects on the electrocatalytic performance of iridium-based nanoparticles for oxygen evolution in rotating disc electrodes. ChemPhysChem 2019;20(22):2956–63. https://doi.org/10.1002/cphc.201900902.

[278] Owe L-E, Tsypkin M, Sunde S. The effect of phosphate on iridium oxide electrochemistry. Electrochim Acta 2011;58:231–7. https://doi.org/10.1016/j.electacta.2011.09.043.

[279] Ganassin A, Colic V, Tymoczko J, Bandarenka AS, Schuhmann W. Non-covalent interactions in water electrolysis: influence on the activity of Pt(111) and iridium oxide catalysts in acidic media. Phys Chem Chem Phys 2015;17(13):8349–55. https://doi.org/10.1039/C4CP04791E. 10.1039/C4CP04791E.

[280] Strickler AL, Higgins D, Jaramillo TF. Crystalline strontium iridate particle catalysts for enhanced oxygen evolution in acid. ACS Appl Energy Mater 2019;2(8):5490–8. https://doi.org/10.1021/acsaem.9b00658.

[281] Alia SM, Rasimick B, Ngo C, Neyerlin KC, Kocha SS, Pylypenko S, Xu H, Pivovar BS. Activity and durability of iridium nanoparticles in the oxygen evolution reaction. J Electrochem Soc 2016;163(11):F3105–12. https://doi.org/10.1149/2.0151611jes.

[282] El-Sayed HA, Weiß A, Olbrich LF, Putro GP, Gasteiger HA. OER catalyst stability investigation using RDE technique: a stability measure or an artifact? J Electrochem Soc 2019;166(8):F458. https://doi.org/10.1149/2.0301908jes.

[283] Geiger S, Kasian O, Mingers AM, Nicley SS, Haenen K, Mayrhofer KJJ, Cherevko S. Catalyst stability benchmarking for the oxygen evolution reaction: the importance of backing electrode material and dissolution in accelerated aging studies. ChemSusChem 2017;10(21):4140–3. https://doi.org/10.1002/cssc.201701523.

[284] Andrews E, Katla S, Kumar C, Patterson M, Sprunger P, Flake J. Electrocatalytic reduction of CO_2@Au nanoparticle electrodes: effects of interfacial chemistry on reduction behavior. J Electrochem Soc 2015;162(12):F1373–8. https://doi.org/10.1149/2.0541512jes.

[285] Edgington J, Deberghes A, Seitz LC. Glassy carbon substrate oxidation effects on electrode stability for oxygen evolution reaction catalysis stability benchmarking. ACS Appl Energy Mater 2022. https://doi.org/10.1021/acsaem.2c01690.

[286] Yang M, Yan S, Du A, Liu J, Xu S. Effect of micro-cracks on the in-plane electronic conductivity of proton exchange membrane fuel cell catalyst layers based on

lattice Boltzmann method. Int J Hydrogen Energy 2022;47(94):39961–72. https://doi.org/10.1016/j.ijhydene.2022.09.142.
[287] Xu, S.; Liu, H.; Zheng, N.; Tao, H. B. Physical degradation of anode catalyst layer in proton exchange membrane water electrolysis. Adv Mater Interfac n/a (n/a), 2400549. DOI: https://doi.org/10.1002/admi.202400549.
[288] Siroma Z, Kakitsubo R, Fujiwara N, Ioroi T, Yamazaki S-i, Yasuda K. Depression of proton conductivity in recast Nafion® film measured on flat substrate. J Power Sources 2009;189(2):994–8. https://doi.org/10.1016/j.jpowsour.2008.12.141.
[289] Morales DM, Villalobos J, Kazakova MA, Xiao J, Risch M. Nafion-induced reduction of manganese and its impact on the electrocatalytic properties of a highly active MnFeNi oxide for bifunctional oxygen conversion. Chemelectrochem 2021;8(15):2979–83. https://doi.org/10.1002/celc.202100744.
[290] McCrory CCL, Jung S, Ferrer IM, Chatman SM, Peters JC, Jaramillo TF. Benchmarking hydrogen evolving reaction and oxygen evolving reaction electrocatalysts for solar water splitting devices. J Am Chem Soc 2015;137(13):4347–57. https://doi.org/10.1021/ja510442p.
[291] Wei C, Xu ZJ. The comprehensive understanding of as an evaluation parameter for electrochemical water splitting. Small Methods 2018;2(11):1800168. https://doi.org/10.1002/smtd.201800168.
[292] Xu J, Lian Z, Wei B, Li Y, Bondarchuk O, Zhang N, Yu Z, Araujo A, Amorim I, Wang Z, et al. Strong electronic coupling between ultrafine iridium–ruthenium nanoclusters and conductive, acid-stable tellurium nanoparticle support for efficient and durable oxygen evolution in acidic and neutral media. ACS Catal 2020;10(6):3571–9. https://doi.org/10.1021/acscatal.9b05611.
[293] McCrory CCL, Jung S, Peters JC, Jaramillo TF. Benchmarking heterogeneous electrocatalysts for the oxygen evolution reaction. J Am Chem Soc 2013;135(45):16977–87. https://doi.org/10.1021/ja407115p.
[294] Spanos I, Auer AA, Neugebauer S, Deng X, Tüysüz H, Schlögl R. Standardized benchmarking of water splitting catalysts in a combined electrochemical flow cell/inductively coupled plasma–optical emission spectrometry (ICP-OES) setup. ACS Catal 2017;7(6):3768–78. https://doi.org/10.1021/acscatal.7b00632.
[295] Peugeot A, Creissen CE, Karapinar D, Tran HN, Schreiber M, Fontecave M. Benchmarking of oxygen evolution catalysts on porous nickel supports. Joule 2021;5(5):1281–300. https://doi.org/10.1016/j.joule.2021.03.022.
[296] Creel EB, Lyu X, McCool G, Ouimet RJ, Serov A. Protocol for screening water oxidation or reduction electrocatalyst activity in a three-electrode cell for alkaline exchange membrane electrolysis. Front Energy Res 2022;10:Methods. https://doi.org/10.3389/fenrg.2022.871604.
[297] Exner KS, Sohrabnejad-Eskan I, Over H. A universal approach to determine the free energy diagram of an electrocatalytic reaction. ACS Catal 2018;8(3):1864–79. https://doi.org/10.1021/acscatal.7b03142.
[298] Exner KS, Over H. Beyond the rate-determining step in the oxygen evolution reaction over a single-crystalline IrO_2(110) model electrode: kinetic scaling relations. ACS Catal 2019;9(8):6755–65. https://doi.org/10.1021/acscatal.9b01564.
[299] Pan X, Du W, Zhao X, Chang G, Zhao Z, Li C, Lei M. Efficient exfoliation method of sodium-ruthenium composites for acid water oxidation. Adv Compos Hybrid Mater 2022;5(3):2536–45. https://doi.org/10.1007/s42114-022-00521-3.
[300] Zhao Y, Hu J, Chiang C-L, Li Y, Yang W, Yang Z, Hung W-H, Lin Y-G, Chen Z, Li B, et al. Ruthenium oxychloride supported by manganese oxide for stable oxygen evolution in acidic media. J Mater Chem A 2022. https://doi.org/10.1039/D2TA05335G. 10.1039/D2TA05335G.
[301] Siracusano S, Baglio V, Van Dijk N, Merlo L, Aricò AS. Enhanced performance and durability of low catalyst loading PEM water electrolyser based on a short-side chain perfluorosulfonic ionomer. Appl Energy 2017;192:477–89. https://doi.org/10.1016/j.apenergy.2016.09.011.
[302] Frydendal R, Paoli EA, Knudsen BP, Wickman B, Malacrida P, Stephens IEL, Chorkendorff I. Benchmarking the stability of oxygen evolution reaction catalysts: the importance of monitoring mass losses. Chemelectrochem 2014;1(12):2075–81. https://doi.org/10.1002/celc.201402262.
[303] Ehelebe K, Schmitt N, Sievers G, Jensen AW, Hrnjić A, Collantes Jiménez P, Kaiser P, Geuß M, Ku Y-P, Jovanovič P, et al. Benchmarking fuel cell electrocatalysts using gas diffusion electrodes: inter-lab comparison and best practices. ACS Energy Lett 2022;7(2):816–26. https://doi.org/10.1021/acsenergylett.1c02659.
[304] Bender G, Carmo M, Smolinka T, Gago A, Danilovic N, Mueller M, Ganci F, Fallisch A, Lettenmeier P, Friedrich KA, et al. Initial approaches in benchmarking and round robin testing for proton exchange membrane water electrolyzers. Int J Hydrogen Energy 2019;44(18):9174–87. https://doi.org/10.1016/j.ijhydene.2019.02.074.
[305] Lickert T, Fischer S, Young JL, Klose S, Franzetti I, Hahn D, Kang Z, Shviro M, Scheepers F, Carmo M, et al. Advances in benchmarking and round robin testing for PEM water electrolysis: reference protocol and hardware. Appl Energy 2023;352:121898. https://doi.org/10.1016/j.apenergy.2023.121898.
[306] Appelhaus S, Ritz L, Pape S-V, Lohmann-Richters F, Kraglund MR, Jensen JO, Massari F, Boroomandnia M, Romanò M, Albers J, et al. Benchmarking performance: a round-robin testing for liquid alkaline electrolysis. Int J Hydrogen Energy 2024;95:1004–10. https://doi.org/10.1016/j.ijhydene.2024.11.288.